

Unearthing the soil carbon food web with DNA-SIP

Ashley N Campbell * †, Charles Pepe-Ranney * ‡, and Daniel H Buckley ‡

*co-first author, †Department of Microbiology, Cornell University, New York, USA, and ‡Department of Crop and Soil Sciences, Cornell University, New York, USA

Submitted to Proceedings of the National Academy of Sciences of the United States of America

Abstract

We describe an approach for identifying microbial contributions to soil C-cycling dynamics using nucleic acid stable isotope probing coupled with next generation sequencing (HR-SIP). We amended three series of soil microcosms with a complex mixture of model carbon (C) substrates and inorganic nutrients similar to plant biomass. A single C constituent in the C substrate mixture was substituted for its ^{13}C -labeled equivalent in two microcosm series. Specifically, in separate microcosms we substituted ^{13}C -xylose or ^{13}C -cellulose for their unlabeled equivalents. Xylose and cellulose were chosen to represent labile soluble C and polymeric insoluble C, respectively. Microcosm DNA was interrogated for ^{13}C incorporation at days 1, 3, 7, 14 and 30. Incorporation of ^{13}C from xylose into microcosm DNA was observed at days 1, 3, and 7, while incorporation of ^{13}C from cellulose was peaked at day 14 and was maintained through day 30. Of over 6,000 OTUs detected, a total of 49 and 63 unique OTUs assimilated ^{13}C from xylose and cellulose into DNA, respectively. Xylose assimilating OTUs were more abundant in the microcosm community than cellulose assimilating OTUs, while cellulose OTUs demonstrated a greater substrate specificity than xylose OTUs.

monolayer | structure | x-ray reflectivity | molecular electronics

Abbreviations: SAM, self-assembled monolayer; OTS, octadecyltrichlorosilane

Introduction

Excluding plant biomass, there are 2,300 Pg of carbon (C) stored in soils worldwide which accounts for ~80% of the global terrestrial C pool [1, 2]. When organic C from plants reaches soil it is degraded by fungi, archaea, and bacteria. The majority of plant biomass C in soil is respiration and produces 10 times more CO_2 annually than anthropogenic emissions [3]. Global changes in atmospheric CO_2 , temperature, and ecosystem nitrogen inputs are expected to impact soil C input [4]. Current climate change models concur on atmospheric and oceanic but not terrestrial C predictions [5]. Contrasting terrestrial C model predictions reflect

how little is known about soil C cycling. Inconsistencies in terrestrial modeling could be improved by elucidating the relationship between dissolved organic C and soil microbial community composition [6].

An important step in understanding soil C cycling dynamics is identifying the *in situ* activity of specific microbial lineages to establish relationship between community structure and function [7]. An estimated 80–90% of soil C cycling is mediated by microorganisms [8, 9] but understanding microbial processing of soil nutrients is challenging due to soil’s heterogeneous nature and methods limitations. The vast majority of microorganisms resist cultivation in the laboratory. Stable-isotope probing (SIP) links microbial identity and activity without cultivation and has expanded our knowledge of microbial contributions to biogeochemical processes [10]. The most successful applications of SIP have identified organisms which mediate processes performed by a narrow set of functional guilds such as methanogens [11]. SIP has been less applicable to the study of soil C cycling because of limitations in resolving power as a result of simultaneous labeling of many different organisms in the community. Additionally, molecular applications such as tRFLP, DGGE and cloning that are frequently used in conjunction with SIP provide insufficient resolution of taxon identity and/or depth of coverage. We developed an approach called High Resolution-SIP (HR-SIP) that employs a complex mixture of substrates added to soil at a low concentration relative to soil organic matter pools along with high throughput DNA sequencing. This greatly expands the ability of nucleic acid SIP to

Reserved for Publication Footnotes

explore complex patterns of C-cycling in microbial communities with increased resolution.

A temporal activity cascade occurs in natural microbial communities during plant biomass degradation in which labile C is degraded before polymeric C [12, 13]. The aim of this study was to observe temporal dynamics of C assimilation through discrete soil community members. Our experimental approach included the addition of a soil organic matter (SOM) simulant (a complex mixture of model carbon sources and inorganic nutrients common to plant biomass) so soil microcosms where a single C component is substituted for its ^{13}C -labeled equivalent. Parallel incubations of soils amended with this complex C mixture allows us to observe how different C substrates move through the soil microbial community. In this study we used ^{13}C -xylose and ^{13}C -cellulose as a proxy for labile and polymeric C, respectively, and coupled nucleic acid stable isotope probing with high throughput DNA sequencing. Amplicon sequencing of 16S rRNA gene fragments from many gradient fractions and multiple gradients make it possible to track C associated activities for hundreds of soil taxa.

Results

We observed C use dynamics in an agricultural soil microbial community by conducting a nucleic acid SIP experiment wherein xylose or cellulose carried the isotopic label. We set up three soil microcosm series. Each microcosm was amended with a C substrate mixture that included cellulose and xylose. The C substrate mixture approximated the chemical composition of fresh plant biomass. The same mixture was added to microcosms in each series, however, for each series except the control, xylose or cellulose was substituted for its ^{13}C counterpart. Microcosm amendments are shorthand identified in figures by the following code: “13CXPS” refers to the amendment with ^{13}C -xylose (that is ^{13}C Xylose Plant Simulant), “13CCPS” refers to the ^{13}C -cellulose amendment and “12CCPS” refers to the amendment that only contained ^{12}C substrates (i.e. control). 5.3 mg of C gram $^{-1}$ soil C substrate mixture was added to each microcosm representing 18% of the soil C. The mixture included 0.42 mg xylose-C and 0.88 mg cellulose-C g soil $^{-1}$. Microcosms were harvested at days 1, 3, 7, 14 and 30 during a 30 day incubation. ^{13}C -xylose assimilation peaked immediately and tapered over the 30 day incubation whereas ^{13}C -cellulose assimilation peaked two weeks after amendment additions (Figure 1).

See Supplemental Note XX for sequencing and density fractionation statistics.

Soil microcosm microbial community changes with time.

Bulk soil DNA SSU rRNA gene amplicon sequencing revealed changes in the soil microcosm microbial community structure and membership correlated significantly with incubation time (Figure S7B, p-value 0.23, R^2 0.63, Adonis test [14]). The identity of the ^{13}C -labeled substrate added to the microcosms did not significantly correlate with community structure and membership (p-value 0.35). Additionally, microcosm beta diversity was significantly less than gradient fraction beta diversity (p-value 0.003, “betadisper” function R Vegan package [15, 16]). Twenty-nine OTUs significantly changed in relative abundance with time (“BH” adjusted p-value <0.10, [17]) (Figure S2). OTUs that significantly increased in relative abundance with time included OTUs in the *Verrucomicrobia*, *Proteobacteria*, *Planctomycetes*, *Cyanobacteria*, *Chloroflexi* and *Actinobacteria*. OTUs that significantly decreased in relative abundance with time included OTUs in the *Proteobacteria*, *Firmicutes*, *Bacteroidetes* and *Actinobacteria* (Figure S2). *Proteobacteria* was the only phylum that had OTUs which increased significantly and OTUs that decreased significantly in abundance with time. If sequences were grouped by taxonomic annotations at the class level, only four classes significantly changed in abundance, *Bacilli* (decreased), *Flavobacteria* (decreased), *Gammaproteobacteria* (decreased) and *Herpetosiphonales* (increased) (Figure S5). Of the 29 OTUs that changed significantly in relative abundance with time, 14 are labeled substrate responders (Figure S2).

Responder abundances summed at phylum level generally increased for ^{13}C -cellulose (Figure S8) whereas ^{13}C -xylose responder abundances summed at the phylum level decreased over time for *Firmicutes*, *Bacteroidetes*, *Actinobacteria* and *Proteobacteria* although *Proteobacteria* spiked at day 14 (Figure S8). Bulk abundance trends are roughly consistent with ^{13}C assimilation.

OTUs that assimilated ^{13}C into DNA. Within the first 7 days of incubation approximately 63% of ^{13}C -xylose was respired and only an additional 6% more was respired from day 7 to 30. At day 30, 30% of the ^{13}C from xylose remained. An average 16% of the ^{13}C -cellulose added was respired within the first 7 days, 38% by day 14, and 60% by day 30.

Isotope incorporation by an OTU is revealed by enrichment of the OTU in heavy CsCl gradient fractions containing ^{13}C labeled DNA relative to heavy fractions from control gradients containing no ^{13}C labeled DNA. We refer to OTUs that putatively incorporated ^{13}C into DNA originally from an isotopically labeled substrate as substrate “re-

sponders”. At day 1, 84% of ^{13}C -xylose responsive OTUs belonged to *Firmicutes*, 11% to *Proteobacteria* and 5% to *Bacteroidetes*. *Firmicutes* responders decreased from 16 OTUs at day 1 to one OTU at day 3 while *Bacteroidetes* responders increased from one OTU at day 1 to 12 OTUs at day 3. The remaining day 3 responders are members of the *Proteobacteria* (26%) and the *Verrucomicrobia* (5%). Day 7 responders were 53% *Actinobacteria*, 40% *Proteobacteria*, and 7% *Firmicutes*. The identities of ^{13}C -xylose responders changed with time. The numerically dominant ^{13}C -xylose responder phylum shifted from *Firmicutes* to *Bacteroidetes* and then to *Actinobacteria* across days 1, 3 and 7 (Figure 2, Figure 3).

Only 2 and 5 OTUs had incorporated ^{13}C from ^{13}C -cellulose at days 3 and 7, respectively. At days 14 and 30 42 and 39 OTUs incorporated ^{13}C from ^{13}C -cellulose into biomass. A *Cellvibrio* and *Sandaracinaceae* OTU assimilated ^{13}C from ^{13}C -cellulose at day 3. Day 7 ^{13}C -cellulose responders included the same *Cellvibrio* responder as day 3, a *Verrucomicrobia* OTU and three *Chloroflexi* OTUs. 50% of Day 14 responders belong to *Proteobacteria* (66% Alpha-, 19% Gamma-, and 14% Beta-) followed by 17% *Planctomycetes*, 14% *Verrucomicrobia*, 10% *Chloroflexi*, 7% *Actinobacteria* and 2% cyanobacteria. *Bacteroidetes* OTUs began to incorporate ^{13}C from cellulose at day 30 (13% of day 30 responders). Other day 30 responding phyla included *Proteobacteria* (30% of day 30 responders; 42% Alpha-, 42% Delta, 8% Gamma-, and 8% Beta-), *Planctomycetes* (20%), *Verrucomicrobia* (20%), *Chloroflexi* (13%) and cyanobacteria (3%). *Proteobacteria*, *Verrucomicrobia*, and *Chloroflexi* had relatively high numbers of responders with strong response across multiple time points (Figure 2).

Ecological strategies of ^{13}C responders. ^{13}C -xylose responders are generally more abundant members based on relative abundance in bulk DNA SSU rRNA gene content than ^{13}C -cellulose responders (Figure 4, p-value 0.00028). However, both abundant and rare OTUs responded to ^{13}C -xylose and ^{13}C -cellulose (Figure 4). For instance, a *Delftia* ^{13}C -cellulose responder is fairly abundant in the bulk samples (“OTU.5”, Table S1). OTU.5 was on average the 13th most abundant OTU in bulk samples. A ^{13}C -xylose responder (“OTU.1040”, Table S2) has a mean relative abundance in bulk samples of 3.57×10^{-5} . Two ^{13}C -cellulose responders were not found in any bulk samples (“OTU.862” and “OTU.1312”, Table S1). Of the 10 most abundant responders, 8 are ^{13}C -xylose responders and

6 of these 8 are consistently among the 10 most abundant OTUs in bulk samples.

Cellulose responders exhibited a greater shift in buoyant density (BD) than xylose responders in response to isotope incorporation (Figure 4, p-value 1.8610×10^{-6}). ^{13}C -cellulose responders shifted on average 0.0163 g mL^{-1} (sd 0.0094) whereas xylose responders shifted on average 0.0097 g mL^{-1} (sd 0.0094). For reference, 100% ^{13}C DNA BD is 0.04 g mL^{-1} greater than the BD of its ^{12}C counterpart. DNA BD increases as its ratio of ^{13}C to ^{12}C increases. An organism that only assimilates C into DNA from a ^{13}C isotopically labeled source, will have a greater $^{13}\text{C}:^{12}\text{C}$ ratio in its DNA than an organism utilizing a mixture of isotopically labeled and unlabeled C sources (see supplemental note XX).

^{13}C -xylose responder estimated *rrn* gene copy number was inversely related time of first response (p-value 2.02×10^{-15} , Figure S1). OTUs that first respond at later time points have fewer estimated *rrn* copy number than OTUs that first respond earlier (Figure S1).

Discussion

Pure culture based studies drove early soil microbial ecology research. Historically important soil isolates included nine genera: *Agrobacterium*, *Alcaligenes*, *Arthrobacter*, *Bacillus*, *Flavobacterium*, *Micromonospora*, *Nocardia*, *Pseudomonas*, and *Streptomyces* ([18] and reviewed by [19]) but culture-independent surveys of soil microbial diversity revealed soil can harbor 5,000 OTUs per half gram of soil [20] and that cultured isolates did not represent *in situ* numerically abundant genera. We recovered almost 6,000 OTUs in this study. Although culturing techniques can produce isolates from diverse soil phylogenetic lineages [21], numerically dominant soil microorganisms are still uncultured and we know little of their ecophysiology [19]. In contrast, DNA-SIP can characterize functional roles for thousands of phylotypes in a single experiment. We found 104 OTUs in an agricultural soil that can incorporate from xylose and/or cellulose into biomass. We also used DNA-SIP to assay substrate specificity and temporal dynamics of C-cycling or soluble and polymeric C degraders. Included in the ^{13}C -xylose and ^{13}C -cellulose responsive OTUs were members of numerically dominant yet functionally uncharacterized soil phylogenetic groups such as *Verrucomicrobia*, *Planctomycetes* and *Chloroflexi*.

Microbial response to isotopic labels. We propose that C added to soil microcosms in this experiment took the following path through the microbial food web (Figure S12): First, labile C such as

xylose was assimilated by fast-growing opportunistic *Firmicutes* spore formers. The remaining labile C and new biomass C was assimilated in succession by slower growing *Bacteroidetes*, *Actinobacteria* and *Proteobacteria* phylotypes that were either tuned to lower C substrate concentrations, were predatory bacteria (e.g. *Agromyces*), and/or were specialized for consuming viral lysate. C from polymeric substrates entered the bacterial community after 14 days. Canonical cellulose degrading bacteria such as *Cellvibrio* degraded cellulose but uncharacterized lineages in the *Chloroflexi*, *Planctomycetes* and *Verrucomicrobia*, specifically the *Spartobacteria*, were also significant contributors to cellulose decomposition.

Ecological strategies of soil microorganisms participating in the decomposition of organic matter.

We assessed the ecology of ^{13}C -responsive OTUs by estimating the *rrn* gene copy number and the BD shift upon labeling for each OTU. *rrn* gene copy number correlates positively with growth rate [22] and BD shift is indicative of substrate specificity (see results). We also observed how ^{13}C -substrate responsive OTUs changed in relative abundance with time in the microcosms and the abundance rank of ^{13}C -substrate responsive OTUs in the bulk DNA. Ecological metrics show ^{13}C -cellulose responsive OTUs grow slower (Figure 4, Figure S1), have greater substrate specificity (Figure 4), and are generally lower abundance than ^{13}C -xylose responsive OTUs (Figure 4). The higher abundance of xylose responders may also be in part due to of their high *rrn* gene copy number resulting in inflated relative abundance per genome. There are only faint ecological differences within the ^{13}C -cellulose responsive OTUs but the combination of *rrn* gene copy number, BD shift, abundance rank and relative abundance change over time is consistent with phylum membership (Figure RADVIZ). ^{13}C -xylose responsive OTU *rrn* gene copy number correlated inversely with the time at which the OTU was first found to incorporate ^{13}C into DNA (Figure 4, Figure S1) suggesting that fast-growing microbes assimilated ^{13}C from xylose before slow growers.

Ecological metrics suggest cellulose degraders are substrate specialists that grow slow and are in low bulk abundance. Labile C responder ecological strategies were more varied perhaps because some ^{13}C labeled microorganisms did not primarily assimilate xylose but became labeled via predatory interactions and/or are saprophytes. ^{13}C -xylose responsive OTUs are generalists, grow faster and are more abundant when compared to ^{13}C -cellulose responders. ^{13}C -xylose responders vary in growth rate and while generally higher abundance than ^{13}C -cellulose responders can also be

low abundance microorganisms. It's not clear whether the observed activity succession from *Firmicutes* to *Bacteroidetes* and finally *Actinobacteria* in response to ^{13}C -xylose addition marks a trophic cascade or functional groups tuned to different resource concentrations or both. Notably, each temporally defined response group clustered phylogenetically suggesting a uniform ecological strategy (Figure S6). It's also clear that some of the non-*Firmicutes* ^{13}C -xylose responders are closely related to known predators (*Agromyces*) and many marine predatory bacteria are members of the *Bacteroidetes* ([23]). Further, *Bacteroidetes* have been implicated as soil predatory bacteria previously [24]. If the temporal dynamics of ^{13}C -xylose incorporation are due to trophic interactions, our results suggest that there are many predatory soil bacteria that consume fast-growing, opportunistic, primary labile C assimilating, gram-positive spore-formers. Hence, trophic interactions among soil bacteria may be of importance in soil C turnover models.

How – or if – phylogenetic composition affects SOM dynamics is an open question [25]. Phylogenetic composition could affect SOM dynamics if SOM transformations were not functionally redundant traits and if biology is rate limiting for key C transformations [25]. Alternatively, even with functional redundancy resource allocation at the cell level can influence SOM fate [25]. It is likely that the ability to carry out soil C transformations are redundant within and between soil microbial communities and that in the mineral soil abiotic factors are rate limiting [25]. Therefore phylogenetic composition in mineral soil likely influences soil C fate as opposed to dynamics. We demonstrate a phylogenetically coherent response to soluble C additions – for instance, most of the initial response to xylose can be attributed to aerobic spore formers. Assuming cellular resource allocation is consistent with phylogeny, it follows then that phylogenetic composition can significantly influence SOM fate. Aerobic spore-formers, for example, are found in different proportions across soil biomes [19] and even within regional agricultural soils CITE Berthrong. If present and abundant, aerobic spore-formers may be primary soluble C decomposers and allocate C in specific quantities into intra and extracellular C components. Further, aerobic spore-formers may have a phylogenetically coherent resistance to predation which could further affect soil C fate. Although, not demonstrated in this study, the allocation of C from soluble, labile pools in a soil without or under conditions not suitable for aerobic spore-formers may be significantly different. Polymeric C, on the other hand, did not show the same phylogenetic coherence as soluble C decomposition in this study. This

suggests that resource allocation among cellulose degraders would not have a single phylogenetic signal and the fate of polymeric C would not be tied to phylogenetic composition. Though cellulose degraders as a whole likely allocate C differently than labile C degraders.

Conclusion. Microorganisms sequester atmospheric C and respire soil organic matter (SOM) influencing climate change on a global scale but we do not know which microorganisms carry out specific soil C transformations. In this experiment microbes from uncharacterized yet ubiquitous and often abundant soil lineages participated in cellulose decomposition. Cellulose C degraders included members of the *Verrucomicrobia* (*Spartobacteria*), *Chloroflexi*, *Bacteroidetes* and *Planctomycetes*. *Spartobacteria* in particular are abundant microorganisms in many soil biomes and often the most abundant *Verrucomicrobia* order in soil. Our results also suggest that members of the *Bacteroidetes* and *Actinobacteria* act in the cascade of labile, soluble C through soil trophic levels possibly as predators. Both points illustrate the complexity of soil C dynamics and fate. The largely phylogenetically coherent ecological groups observed in this study suggest that soil C fate is tied to phylogenetic composition.

Methods

Additional information on sample collection and analytical methods is provided in SI Materials and Methods.

Twelve soil cores (5 cm diameter x 10 cm depth) were collected from six random sampling locations within an organically managed agricultural field in Penn Yan, New York. Soils were pretreated by sieving (2 mm), homogenizing sieved soil, and pre-incubating 10 g of dry soil weight in flasks for 2 weeks. Soils were amended with a 5.3 mg g soil⁻¹ carbon mixture; representative of natural concentrations [26]. Mixture contained 38% cellulose, 23% lignin, 20% xylose, 3% arabinose, 1% galactose, 1% glucose, and 0.5% mannose by mass, with the remaining 13.5% mass composed of an amino acid (in-house made replica of Teknova C0705) and basal salt mixture (Murashige and Skoog, Sigma Aldrich M5524). Three parallel treatments were performed; (1) unlabeled control, (2)¹³C-cellulose, (3)¹³C-xylose (98 atom% ¹³C, Sigma Aldrich). Each treatment had 2 replicates per time point (n = 4) except day 30 which had 4 replicates; total microcosms per treatment n = 12, except ¹³C-cellulose which was not sampled at day 1, n = 10. Other details relating to substrate addition can be found in SI. Microcosms were sampled destructively (stored at -80°C until nucleic acid pro-

cessing) at days 1 (control and xylose only), 3, 7, 14, and 30.

Nucleic acids were extracted using a modified Griffiths protocol [27]. To prepare nucleic acid extracts for isopycnic centrifugation as previously described [28], DNA was size selected (>4kb) using 1% low melt agarose gel and β -agarase I enzyme extraction per manufacturers protocol (New England Biolab, M0392S). For each time point in the series isopycnic gradients were setup using a modified protocol [29] for a total of five ¹²C-control, five ¹³C-xylose, and four ¹³C-cellulose microcosms. A density gradient (average density 1.69 g mL⁻¹) solution of 1.762 g cesium chloride (CsCl) mL⁻¹ in gradient buffer solution (pH 8.0 15 mM Tris-HCl, 15 mM EDTA, 15 mM KCl) was used to separate ¹³C-enriched and ¹²C-nonenriched DNA. Each gradient was loaded with approximately 5 μ g of DNA and ultracentrifuged for 66 h at 55,000 rpm and room temperature (RT). Fractions of ~100 μ L were collected from below by displacing the DNA-CsCl-gradient buffer solution in the centrifugation tube with water using a syringe pump at a flow rate of 3.3 μ L s⁻¹ [30] into AcroprepTM 96 filter plate (Pall Life Sciences 5035). The refractive index of each fraction was measured using a Reichart AR200 digital refractometer modified as previously described [28] to measure a volume of 5 μ L. Then buoyant density was calculated from the refractive index as previously described [28] (see also SI). The collected DNA fractions were purified by repetitive washing of Acroprep filter wells with TE. Finally, 50 μ L TE was added to each fraction then resuspended DNA was pipetted off the filter into a new microfuge tube.

For every gradient, 20 fractions were chosen for sequencing between the density range 1.67-1.75 g mL⁻¹. Barcoded 454 primers were designed using 454-specific adapter B, 10 bp barcodes [31], a 2 bp linker (5'-CA-3'), and 806R primer for reverse primer (BA806R); and 454-specific adapter A, a 2 bp linker (5'-TC-3'), and 515F primer for forward primer (BA515F). Each fraction was PCR amplified using 0.25 μ L 5 U μ l⁻¹ AmpliTaq Gold (Life Technologies, Grand Island, NY; N8080243), 2.5 μ L 10X Buffer II (100 mM Tris-HCl, pH 8.3, 500 mM KCl), 2.5 μ L 25 mM MgCl₂, 4 μ L 5 mM dNTP, 1.25 μ L 10 mg mL⁻¹ BSA, 0.5 μ L 10 μ M BA515F, 1 μ L 5 μ M BA806R, 3 μ L H₂O, 10 μ L 1:30 DNA template) in triplicate. Samples were normalized either using Pico green quantification and manual calculation or by SequalPrepTM normalization plates (Invitrogen, Carlsbad, CA; A10510), then pooled in equimolar concentrations. Pooled DNA was gel extracted from a 1% agarose gel using Wizard SV gel and PCR clean-up system (Promega, Madison, WI; A9281) per manufacturer's protocol. Amplicons were sequenced

on Roche 454 FLX system using titanium chemistry at Selah Genomics (formerly EnGenCore, Columbia, SC)

Supplemental Notes

Phylogenetic affiliation of ^{13}C -cellulose and ^{13}C -xylose responsive microorganisms. *Proteobacteria* represent 46% of all ^{13}C -cellulose responding OTUs identified. *Cellvibrio* accounted for 3% of all proteobacterial ^{13}C -cellulose responding OTUs detected. *Cellvibrio* was one of the first identified cellulose degrading bacteria and was originally described by Winogradsky in 1929 who named it for its cellulose degrading abilities [32]. All ^{13}C -cellulose responding *Proteobacteria* share high sequence identity with 16S rRNA genes from sequenced cultured isolates (Table S1) except for “OTU.442” (best cultured isolate match 92% sequence identity in the *Chromomyces* genus, Table S1) and “OTU.663” (best cultured isolate match outside *Proteobacteria* entirely, *Clostridium* genus, 89% sequence identity, Table S1). Some *Proteobacteria* responders share high sequence identity with isolates in genera known to possess cellulose degraders including *Rhizobium*, *Devasia*, *Stenotrophomonas* and *Cellvibrio*. One *Proteobacteria* OTU shares high sequence identity (100%) with a *Brevundimonas* cultured isolate. *Brevundimonas* has not previously been identified as a cellulose degrader, but has been shown to degrade celloburonic acid, an oxidized form of cellulose [33].

Verrucomicrobia, a cosmopolitan soil phylum often found in high abundance [34], are hypothesized to degrade polysaccharides in many environments [34–36]. *Verrucomicrobia* comprise 16% of the total ^{13}C -cellulose responder OTUs detected. 40% of *Verrucomicrobia* ^{13}C -cellulose responders belong to the uncultured “FukuN18” family originally identified in freshwater lakes [37]. The strongest *Verrucomicrobial* responder OTU to ^{13}C -cellulose shared high sequence identity (97%) with an isolate from Norway tundra soil [38] although growth on cellulose was not assessed for this isolate. Only one other ^{13}C -cellulose responding verrucomicrobium shared high DNA sequence identity with an isolate, “OTU.638” (Table S1) with *Roseimicrobium gellanilyticum* (100% sequence identity) which has been shown to grow on soluble cellulose [39]. The remaining ^{13}C -cellulose *Verrucomicrobia* responders did not share high sequence identity with any isolates (maximum sequence identity with any isolate 93%).

Chloroflexi are known for metabolically dynamic lifestyles ranging from anoxygenic phototrophy to organohalide respiration [40]. Recent studies have

focused on *Chloroflexi* roles in C cycling [40–42] and several *Chloroflexi* utilize cellulose [40–42]. Four closely related OTUs in an undescribed *Chloroflexi* lineage (closest matching isolate for all four OTUs: *Herpetosiphon geysericola*, 89% sequence identity, Table S1) responded to ^{13}C -cellulose (Figure S6). One additional OTU also from a poorly characterized *Chloroflexi* lineage (closest cultured isolate matched a proteobacterium at 78% sequence identity) responded to ^{13}C -cellulose (Figure S6).

Other notable ^{13}C -cellulose responders include a *Bacteroidetes* OTU that shares high sequence identity (99%) to *Sporocytophaga myxococcoïdes* a known cellulose degrader [43], and three *Actinobacteria* OTUs that share high sequence identity (100%) with isolates. One of the three *Actinobacteria* ^{13}C -cellulose responders is in the *Streptomyces*, a genus known to possess cellulose degraders, while the other two share high sequence identity to cultured isolates *Allokutznizeriz albata* [44, 45] and *Lentzea waywayandensis* [46, 47]; neither isolate decomposes cellulose in culture. Nine *Planctomycetes* OTUs responded to ^{13}C -cellulose but none are within described genera (closest cultured isolate match 91% sequence identity, Table S1) (Figure S6). One ^{13}C -cellulose responder is annotated as “cyanobacteria”. The cyanobacteria phylum annotation is misleading as the OTU is not closely related to any oxygenic phototrophs (closest cultured isolate match *Vampirovibrio chlorellavorus*, 95% sequence identity, Table S1). A sister clade to the oxygenic phototrophs classically annotated as “cyanobacteria” in SSU rRNA gene reference databases, but does not possess any known phototrophs, has recently been proposed to constitute its own phylum, “Melainabacteria” (**author?**) [48]; although, the phylogenetic position of “Melainabacteria” is debated [49]. The catalog of metabolic capabilities associated with cyanobacteria (or candidate phyla previously annotated as cyanobacteria) are quickly expanding [48, 49]. Our findings provide evidence for cellulose degradation within a lineage closely related to but apart from oxygenic phototrophs. Notably, polysaccharide degradation is suggested by an analysis of a “Melainabacteria” genome [48]. Although we highlight ^{13}C -cellulose responders that share high sequence identity with described genera, most ^{13}C -cellulose responders uncovered in this experiment are not closely related to cultured isolates (Table S1).

Verrucomicrobia, cosmopolitan soil microbes [50], can comprise up to 23% of 16S rRNA gene sequences in high-throughput DNA sequencing surveys of SSU rRNA genes in soil [50] and can account for up to 9.8% of soil 16S rRNA [51]. Many *Verrucomicrobia* were first isolated in the last

decade [52] but only one of the 15 most abundant verrucomicrobial phylotypes in a global soil sample collection shared greater than 93% sequence identity with a cultured isolate [50]. Genomic analyses and physiological profiling of *Verrucomicrobia* isolates revealed *Verrucomicrobia* are capable of methanotrophy, diazotrophy, and cellulose degradation [39, 52], yet the function of soil *Verrucomicrobia* in global C-cycling remains unknown. Only two of the ten putative cellulose degrading *Verrucomicrobia* identified in this experiment share at least 95% sequence identity with an isolate (“OTU.83” and “OTU.627”, Table S1). Seven of ten ^{13}C -cellulose responding verrucomicrobial OTUs were classified as *Spartobacteria* which are a numerically dominant family of *Verrucomicrobia* in SSU rRNA gene surveys of 181 globally distributed soil samples [50]. Given their ubiquity and abundance in soil as well as their demonstrated incorporation of ^{13}C from ^{13}C -cellulose, *Verrucomicrobia* lineages, particularly *Spartobacteria*, may be important contributors to cellulose decomposition on a global scale.

Cellulose degrading soil *Chloroflexi* have previously been identified in DNA-SIP studies [53]. The cellulose degrading *Chloroflexi* in this study are only distantly related to isolates S1. *Chloroflexi* are among the six most abundant soil phyla commonly recovered soil microbial diversity surveys [19]. *Chloroflexi* are typically not as abundant as *Verrucomicrobia* but are roughly as abundant as *Bacteroidetes* and *Planctomycetes* [19]. Four of five ^{13}C -cellulose responsive *Chloroflexi* identified in this study are annotated as belonging to the *Herpetosiphon* although they share less than 95% sequence identity with their closest cultured relative in the *Herpetosiphon* genus (*H. geysericola*). *H. geysericola* is a predatory bacterium shown to prey upon *Aerobacter* in culture and can also digest cellulose [54]. In our study, “*Herpetosiphon*” ^{13}C -cellulose responders did not show a delayed response to ^{13}C -cellulose as compared to other responders but nonetheless could have become labeled by feeding on primary ^{13}C -cellulose degraders. The prey specificity of predatory bacteria is not well established especially *in situ*. ^{13}C -labeling would be positively correlated with prey specificity. If the predator specifically preyed upon one population then it could take on the same labeling percent as that population given enough generations. Preying on multiple types would produce a mixed and dilute labeling signature if some of the prey were not isotopically labeled.

We also observed ^{13}C -incorporation from cellulose by *Proteobacteria*, *Planctomycetes* and *Bacteroidetes*. Strains in *Proteobacteria*, *Planctomycetes* and *Bacteroidetes* have all been previously implicated in cellulose degradation. *Plancto-*

mycetes is the least studied of the three phyla and only one *Planctomycetes* isolate can grow on cellulose. None of the seven *Planctomycetes* cellulose degraders identified in this experiment are closely related to isolates. *Acidobacteria* did not pass or operational criteria for assessing ^{13}C incorporation from cellulose into DNA in our microcosms. *Acidobacteria* have been found to degrade cellulose in culture CITE and are a numerically significant soil phylum CITE. *Acidobacteria* have been shown to dominate at low nutrient availability (CITE: cederlund 2014), which may explain why they were not active upon nutrient additions. The *Acidobacteria* in our microcosms were mainly annotated as belonging to candidate orders in the Silva taxonomic nomenclature. The highest relative abundance for any *Acidobacteria* order in the bulk samples was 0.20 (order “DA023”) and the highest relative abundance of the *Acidobacteria* phylum was 0.23.

All of the ^{13}C -xylose responders in the *Firmicutes* phylum are closely related (at least 99% sequence identity) to cultured isolates from genera that are known to form endospores (Table S2). Each ^{13}C -xylose responder is closely related to isolates annotated as members of *Bacillus*, *Paenibacillus* or *Lysinibacillus*. *Bacteroidetes* ^{13}C -xylose responders are predominantly closely related to *Flavobacterium* species (5 of 8 total responders) (Table S2). Only one *Bacteroidetes* ^{13}C -xylose responder is not closely related to a cultured isolate, “OTU.183” (closest LTP BLAST hit, *Chitinophaga* sp., 89.5% sequence identity, Table S2). OTU.183 shares high sequence identity with environmental clones derived from rhizosphere samples (accession AM158371, unpublished) and the skin microbiome (accession JF219881, (author?) [55]). Other *Bacteroidetes* responders share high sequence identities with canonical soil genera including *Dyadobacter*, *Solibius* and *Terrimonas*. Six of the 8 *Actinobacteria* ^{13}C -xylose responders are in the *Micrococcales* order. One ^{13}C -xylose responding *Actinobacteria* OTU shares 100% sequence identity with *Agromyces ramosus* (Table S2). *A. ramosus* is a known predatory bacterium but is not dependent on a host for growth in culture [56]. It is not possible to determine the specific origin of assimilated ^{13}C in a DNA-SIP experiment. ^{13}C can be passed down through trophic levels although heavy isotope representation in C pools targeted by cross-feeders and predators would be diluted with depth into the trophic cascade. It is possible, however, that the ^{13}C labeled *Agromyces* OTU was assimilating ^{13}C primarily by predation if the *Agromyces* OTU was selective enough with respect to its prey that it primarily attacked ^{13}C -xylose assimilating organisms.

Phylogenetic breadth of ecological strategies. It has been proposed that ecological strategies of soil microorganisms correlate to broad taxonomic groupings CITE (Evans, Schimel, Fierer). Our results suggest that while substrate utilization is not defined at the level of OTU, it is also not defined at the phylum or even family level. Ecology captured at broad phylogenetic breadth would indicate that phylogenetic composition would change in response to changing conditions whereas if ecology is defined by high resolution groups, it suggests that community ecology can change without a corresponding change in composition or specifically that extant taxa would rapidly adapt to environmental change CITE. We found that substrate utilization is captured by phylogenetic levels somewhere between the genus and phylum level (Figure S6). Our measurements did define differences between and within substrate responder groups suggesting there are ecological strategy sub-groups within larger groups defined by an affinity for a particular substrate (Figure 4, Figure S1). Hence, compositional changes could occur at different phylogenetic scales in response to environmental perturbation.

Buoyant density shift estimates. Upon labeling, DNA from an organism that incorporates exclusively ^{13}C will increase in BD more than DNA from an organism that does not exclusively utilize isotopically labeled C. Therefore the magnitude DNA BD shifts indicate substrate specificity given our experimental design as only one substrate was labeled in each amendment. We measured density shift as the change in an OTU’s density profile center of mass between corresponding control and labeled gradients. BD shifts, however, should not be evaluated on an individual OTU basis as a small number of density shifts are observed for each OTU and the variance of the density shift metric at the level of individual OTUs is unknown. It is therefore more informative to compare density shifts among substrate responder groups. Further, density shifts are based on relative abundance profiles and would be distorted in comparison to density shifts based on absolute abundance profiles and should be interpreted with this transformation in mind. It should also be noted that there was overlap in observed density shifts between ^{13}C -cellulose and ^{13}C -xylose responder groups, suggesting that although cellulose degraders are generally more substrate specific than xylose utilizers, each responder group exhibits a range of substrate specificities (Figure 4).

***rrn* gene copy number.** *rrn* copy number estimation is a recent advance in microbiome science [57] although the relationship of *rrn* copy number per

genome with ecological strategy is well established [58]. Microorganisms with a high *rrn* copy number tend to be fast growers specialized to take advantage of boom-bust environments whereas microorganisms with low *rrn* copy number favor slower growth under lower and more consistent nutrient input [58]. At the beginning of our incubation, OTUs with estimated high *rrn* copy number or “fast-growers” assimilate xylose into biomass and with time slower growers (lower *rrn* copy number) begin to incorporate ^{13}C from xylose. Further, ^{13}C -xylose responders have more estimated rRNA operon copy numbers per genome than ^{13}C -cellulose responders ($p\text{-value } 1.878 \times 10^{-09}$) suggesting xylose respiring microbes are generally faster growers than cellulose degraders.

Sequencing statistics and density fractionation. Microcosm DNA was density fractionated on CsCl density gradients. We sequenced SSU rRNA gene amplicons from a total of 277 CsCl gradient fractions from 14 CsCl gradients and 12 bulk microcosm DNA samples. The SSU rRNA gene data set contained 1,102,685 total sequences. The average number of sequences per sample was 3,816 (sd 3,629) and 265 samples had over 1,000 sequences. We sequenced SSU rRNA gene amplicons from an average of 19.8 fractions per CsCl gradient (sd 0.57). The average density between fractions was 0.0040 g mL $^{-1}$. The sequencing effort recovered a total of 5,940 OTUs. 2,943 of the total 5,940 OTUs were observed in bulk samples. We observed 33 unique phylum and 340 unique genus annotations.

References

1. Amundson R (2001) The carbon budget in soils. *Annu Rev Earth Planet Sci* 29(1): 535–562.
2. Batjes N-H (1996) Total carbon and nitrogen in the soils of the world. *European Journal of Soil Science* 47(2): 151–163.
3. Chapin F (2002) Principles of terrestrial ecosystem ecology.
4. Groenigen K-J, Graaff M-A, Six J, Harris D, Kuikman P, Kessel C (2006) The impact of elevated atmospheric CO₂ on soil C and N dynamics: a meta-analysis. *Managed Ecosystems and CO₂* (Springer Science, Berlin Heidelberg), pp 373–391.
5. Friedlingstein P, Cox P, Betts R, Bopp L, von W-B, Brovkin V, Cadule P, Doney S, Eby M, Fung I, et al. (2006) Climate–carbon cycle feedback analysis: Results from the C4 model intercomparison. *J Climate* 19(14): 3337–3353.
6. Neff J-C, Asner G-P (2001) Dissolved organic carbon in terrestrial ecosystems: synthesis and a model. *Ecosystems* 4(1): 29–48.

7. O'Donnell A-G, Seasman M, Macrae A, Waite I, Davies J-T (2002) Plants and fertilisers as drivers of change in microbial community structure and function in soils. *Interactions in the Root Environment: An Integrated Approach* (Springer, Netherlands), pp 135–145.
8. Coleman D-C, Crossley D-A (1996) Fundamentals of Soil Ecology.
9. Nannipieri P, Ascher J, Ceccherini M-T, Landi L, Pietramellara G, Renella G (2003) Microbial diversity and soil functions. *European Journal of Soil Science* 54(4): 655–670.
10. Chen Y, Murrell J-C (2010) When metagenomics meets stable-isotope probing: progress and perspectives. *Trends Microbiol* 18(4): 157–163.
11. Lu Y (2005) In situ stable isotope probing of methanogenic archaea in the rice rhizosphere. *Science* 309(5737): 1088–1090.
12. Hu S, van Bruggen A-HC (1997) Microbial dynamics associated with multiphasic decomposition of ¹⁴C-Labeled Cellulose in Soil. *Microb Ecol* 33(2): 134–143.
13. Rui J, Peng J, Lu Y (2009) Succession of bacterial populations during plant residue decomposition in rice field soil. *Appl Environ Microbiol* 75(14): 4879–4886.
14. Anderson M-J (2001) A new method for non-parametric multivariate analysis of variance. *Austral Ecology* 26(1): 32–46.
15. Anderson M-J, Ellingsen K-E, McArdle B-H (2006) Multivariate dispersion as a measure of beta diversity. *Ecology Letters* 9(6): 683–693.
16. Oksanen J, Kindt R, Legendre P, OHara B, Stevens M-HH, Oksanen M-J, Suggs M (2007) The vegan package.
17. Benjamini Y, Hochberg Y (1995) Controlling the false discovery rate: a practical and powerful approach to multiple testing. *Journal of the Royal Statistical Society, Series B* 57(1): 289–300.
18. Alexander M (1977) Introduction to Soil Microbiology.
19. Janssen P-H (2006) Identifying the dominant soil bacterial taxa in libraries of 16S rRNA and 16S rRNA genes. *Appl Environ Microbiol* 72(3): 1719–1728.
20. Schloss P-D, Handelsman J (2006) Toward a census of bacteria in soil. *PLoS Comput Biol* 2(7): eprint.
21. Janssen P-H, Yates P-S, Grinton B-E, Taylor P-M, Sait M (2002) Improved culturability of soil bacteria and isolation in pure culture of novel members of the divisions acidobacteria, actinobacteria, proteobacteria, and verrucomicrobia. *Applied and Environmental Microbiology* 68(5): 2391–2396.
22. Klappenbach J, Saxman P, Cole J, Schmidt T (2001) rrndb: the Ribosomal RNA Operon Copy Number Database.. *Nucleic Acids Res* 29(1): 181–184.
23. Banning E-C, Casciotti K-L, Kujawinski E-B (2010) Novel strains isolated from a coastal aquifer suggest a predatory role for flavobacteria. *FEMS Microbiol Ecol* 73(2): 254–270.
24. Lueders T, Kindler R, Miltner A, Friedrich M-W, Kaestner M (2006) Identification of Bacterial Micropredators Distinctively Active in a Soil Microbial Food Web. *Appl Environ Microbiol* 72(8): 5342–5348.
25. Schimel J-P, Schaeffer S-M (2012) Microbial control over carbon cycling in soil. *Frontiers in Microbiology* 3: 348. doi: 10.3389/fmicb.2012.00348
26. Schneckenberger K, Demin D, Stahr K, Kuzyakov Y (2008) Microbial utilization and mineralization of ¹⁴C glucose added in six orders of concentration to soil. *Soil Biology and Biochemistry* 40(8): 1981–1988.
27. Griffiths R-I, Whiteley A-S, O'Donnell A-G, Bailey M-J (2000) Rapid method for coextraction of DNA and RNA from natural environments for analysis of ribosomal DNA- and rRNA-based microbial community composition. *Appl Environ Microbiol* 66(12): 5488–5491.
28. Buckley D-H, Huangyutitham V, Hsu S-F, Nelson T-A (2007) Stable isotope probing with ¹⁵N achieved by disentangling the effects of genome G+C content and isotope enrichment on dna Density. *Appl Environ Microbiol* 73(10): 3189–3195.
29. Neufeld J-D, Vohra J, Dumont M-G, Lueders T, Manefield M, Friedrich M-W, Murrell J-C (2007) DNA stable-isotope probing. *Nature Protocols* 2(4): 860–866.
30. Manefield M, Whiteley A-S, Griffiths R-I, Bailey M-J (2002) RNA Stable isotope probing a novel means of linking microbial community function to phylogeny. *Appl Environ Microbiol* 68(11): 5367–5373.
31. Hamady M, Walker J-J, Harris J-K, Gold N-J, Knight R (2008) Error-correcting barcoded primers for pyrosequencing hundreds of samples in multiplex. *Nat Meth* 5(3): 235–237.
32. Boone D (2001) Bergey's manual of systematic bacteriology.
33. Tavernier M-L, Delattre C, Petit E, Michaud P (2008) β -(1,4)-Polyglucuronic Acids - An Overview. *TOBIOTJ* 2(1): 73–86.
34. Fierer N, Ladau J, Clemente J-C, Leff J-W, Owens S-M, Pollard K-S, Knight R, Gilbert J-A, McCulley R-L (2013) Reconstructing the microbial diversity and function of pre-agricultural tallgrass prairie soils in the united

- states. *Science* 342(6158): 621–624.
35. Herlemann D-PR, Lundin D, Labrenz M, Jurgens K, Zheng Z, Aspeborg H, Andersson A-F (2013) Metagenomic de novo assembly of an aquatic representative of the verrucomicrobial class spartobacteria. *mBio* 4(3): e0056912.
 36. Chin K-J, Hahn D, Hengstmann U, Liesack W, Janssen P-H (1999) Characterization and identification of numerically abundant culturable bacteria from the anoxic bulk soil of rice paddy microcosms. *Appl Environ Microbiol* 65(11): 5042–5049.
 37. Parveen B, Mary I, Velle A, Ravet V, Debroas D (2013) Temporal dynamics and phylogenetic diversity of free-living and particle-associated Verrucomicrobia communities in relation to environmental variables in a mesotrophic lake. *FEMS Microbiol Ecol* 83(1): 189–201.
 38. Jiang F, Li W, Xiao M, Dai J, Kan W, Chen L, Li W, Fang C, Peng F (2011) Luteolibacter luojiensis sp. nov. isolated from Arctic tundra soil, and emended description of the genus Luteolibacter. *Int J Syst Evol Microbiol* 62(Pt 9): 2259–2263.
 39. Otsuka S, Ueda H, Suenaga T, Uchino Y, Hamada M, Yokota A, Senoo K (2012) Roseimicrobium gellanilyticum gen. nov. sp. nov., a new member of the class Verrucomicrobiae. *Int J Syst Evol Microbiol* 63(Pt 6): 1982–1986.
 40. Hug L-A, Castelle C-J, Wrighton K-C, Thomas B-C, Sharon I, Frischkorn K-R, Williams K-H, Tringe S-G, Banfield J-F (2013) Community genomic analyses constrain the distribution of metabolic traits across the Chloroflexi phylum and indicate roles in sediment carbon cycling. *Microbiome* 1(1): 22.
 41. Goldfarb K-C, Karaoz U, Hanson C-A, Santee C-A, Bradford M-A, Treseder K-K, Wallenstein M-D, Brodie E-L (2011) Differential Growth Responses of Soil Bacterial Taxa to Carbon Substrates of Varying Chemical Recalcitrance. *Frontiers in Microbiology* 2: 94. doi: 10.3389/fmicb.2011.00094
 42. Cole J-K, Gieler B-A, Heisler D-L, Palisoc M-M, Williams A-J, Dohnalkova A-C, Ming H, Yu T-T, Dodsworth J-A, Li W-J, et al. (2013) Kallotenuus papyrolyticum gen. nov. sp. nov., a cellulolytic and filamentous thermophile that represents a novel lineage (Kallotenuales ord. nov., Kallotenuaceae fam. nov.) within the class Chloroflexia. *Int J Syst Evol Microbiol* 63(Pt 12): 4675–4682.
 43. Vance I, Topham C-M, Blayden S-L, Tamplin J (1980) Extracellular Cellulase Production by Sporocytophaga myxococcoides NCIB 8639. *Microbiology* 117(1): 235–241.
 44. Labeda D-P, Kroppenstedt R-M (2008) Proposal for the new genus Allokutzneria gen. nov. within the suborder Pseudonocardineae and transfer of Kibdelosporangium albatum Tomita et al. 1993 as Allokutzneria albata comb. nov.. *Int J Syst Evol Microbiol* 58(6): 1472–1475.
 45. Tomita K, Hoshino Y, Miyaki T (1993) Kibdelosporangium albatum sp. nov. Producer of the Antiviral Antibiotics Cycloviracins. *Int J Syst Bacteriol* 43(2): 297–301.
 46. Labeda D-P, Lyons A-J (1989) Saccharothrix texensis sp. nov. and Saccharothrix waywayensis sp. nov.. *Int J Syst Bacteriol* 39(3): 355–358.
 47. Labeda D-P, Hatano K, Kroppenstedt R-M, Tamura T (2001) Revival of the genus Lentzea and proposal for Lechevalieria gen. nov. *Int J Syst Evol Microbiol* 51(3): 1045–1050.
 48. Rienzi S-CD, Sharon I, Wrighton K-C, Koren O, Hug L-A, Thomas B-C, Goodrich J-K, Bell J-T, Spector T-D, Banfield J-F, et al. (2013) The human gut and groundwater harbor non-photosynthetic bacteria belonging to a new candidate phylum sibling to Cyanobacteria. *eLIFE* 2: e01102.
 49. Soo R-M, Skennerton C-T, Sekiguchi Y, Imelfort M, Paech S-J, Dennis P-G, Steen J-A, Parks D-H, Tyson G-W, Hugenholtz P (2014) An expanded genomic representation of the phylum cyanobacteria. *Genome Biology and Evolution* 6(5): 1031–1045.
 50. Bergmann G-T, Bates S-T, Eilers K-G, Lauber C-L, Caporaso J-G, Walters W-A, Knight R, Fierer N (2011) The under-recognized dominance of Verrucomicrobia in soil bacterial communities. *Soil Biology and Biochemistry* 43(7): 1450–1455.
 51. Buckley D-H, Schmidt T-M (2001) Environmental factors influencing the distribution of rRNA from Verrucomicrobia in soil. *FEMS Microbiol Ecol* 35(1): 105–112.
 52. Wertz J-T, Kim E, Breznak J-A, Schmidt T-M, Rodrigues J-LM (2011) Genomic and physiological characterization of the verrucomicrobia isolate diplosphaera colitermitum gen. nov. sp. nov., reveals microaerophily and nitrogen fixation genes. *Appl Environ Microbiol* 78(5): 1544–1555.
 53. Schellenberger S, Kolb S, Drake H-L (2010) Metabolic responses of novel cellulolytic and saccharolytic agricultural soil Bacteria to oxygen. *Environ Microbiol* 12(4): 845–861.
 54. Lewin R-A (1970) New Herpetosiphon species (Flexibacterales). *Canadian Journal of Microbiology* 16(6): 517–520.
 55. Kong H-H, Oh J, Deming C, Conlan S, Grice E-A, Beatson M-A, Nomicos E, Polley E-C, Komarow H-D, Murray P-R, et al. (2012) Temporal shifts in the skin microbiome associated



- with disease flares and treatment in children with atopic dermatitis. *Genome Res* 22(5): 850–859.
56. Casida L-E (1983) Interaction of Agromyces ramosus with Other Bacteria in Soil.. *Appl Environ Microbiol* 46(4): 881–888.
57. Kembel S-W, Wu M, Eisen J-A, Green J-L (2012) Incorporating 16S gene copy number information improves estimates of microbial diversity and abundance. *PLoS Comput Biol* 8(10): e1002743.
58. Klappenbach J-A, Dunbar J-M, Schmidt T-M (2000) rRNA Operon copy number reflects ecological strategies of bacteria. *Appl Environ Microbiol* 66(4): 1328–1333.

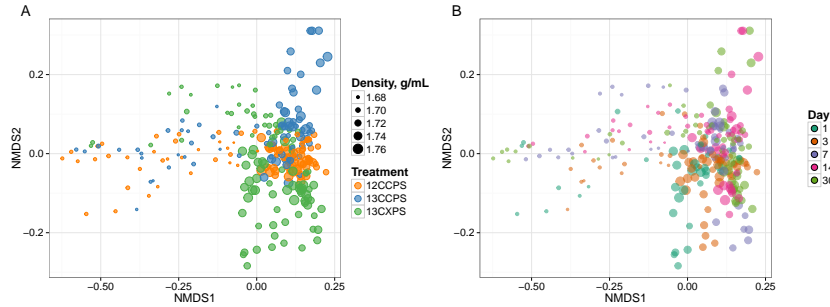


Fig. 1. NMDS analysis from weighted unifrac distances of 454 sequence data from SIP fractions of each treatment over time. Twenty fractions from a CsCl gradient fractionation for each treatment at each time point were sequenced (Fig. S1). Each point on the NMDS represents the bacterial composition based on 16S sequencing for a single fraction where the size of the point is representative of the density of that fraction and the colors represent the treatments (A) or days (B).

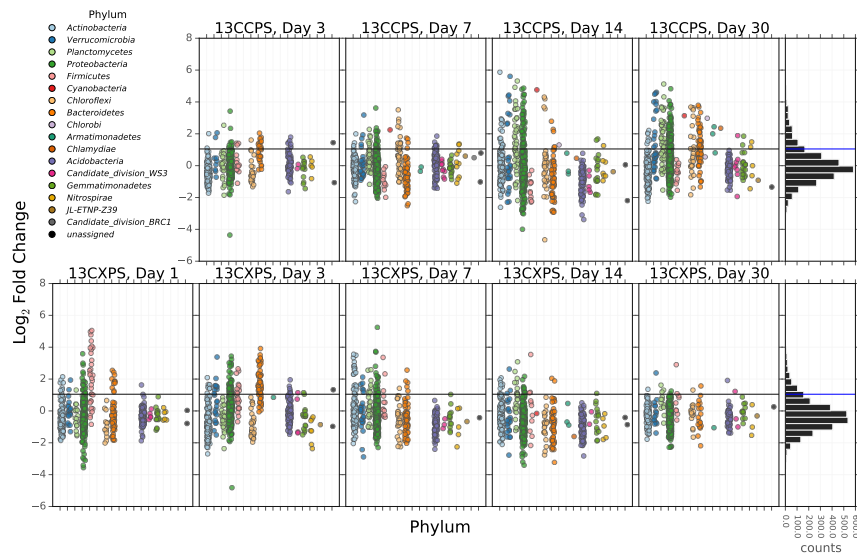


Fig. 2. Log₂ fold change of ¹³C-responders in cellulose treatment (top) and xylose treatment (bottom). Log₂ fold change is based on the relative abundance in the experimental treatment compared to the control within the density range 1.7125–1.755 g ml⁻¹. Taxa are colored by phylum. ‘Counts’ is a histogram of log₂ fold change values.

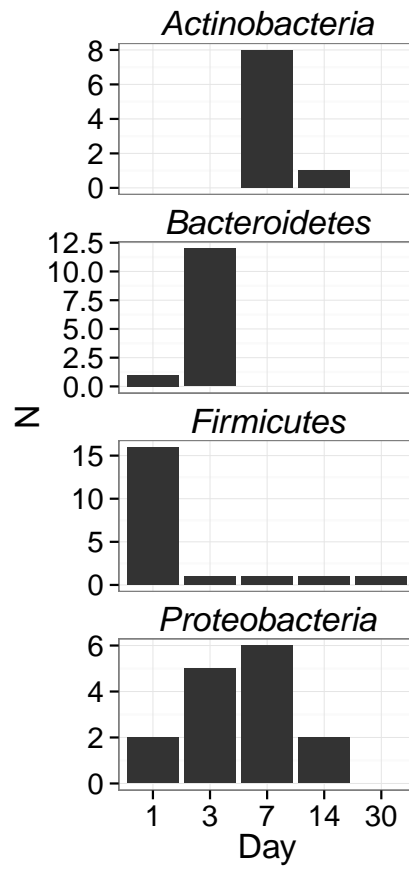


Fig. 3. Counts of ^{13}C -xylose responders in the *Actinobacteria*, *Bacteroidetes*, *Firmicutes* and *Proteobacteria* at days 1, 3, 7 and 30.

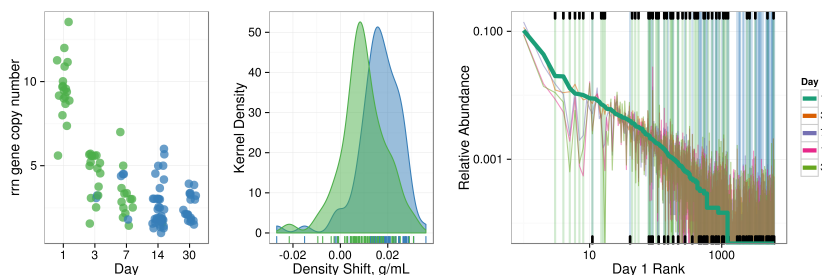


Fig. 4. ^{13}C -responder characteristics based on density shift (A) and rank (B). Kernel density estimation of ^{13}C -responder's density shift in cellulose treatment (blue) and xylose treatment (green) demonstrates degree of labeling for responders for each respective substrate. ^{13}C -responders in rank abundance are labeled by substrate (cellulose, blue; xylose, green). Ticks at top indicate location of ^{13}C -xylose responders in bulk community. Ticks at bottom indicate location of ^{13}C -cellulose responders in bulk community. OTU rank was assessed from day 1 bulk samples.

Supplemental Figures and Tables

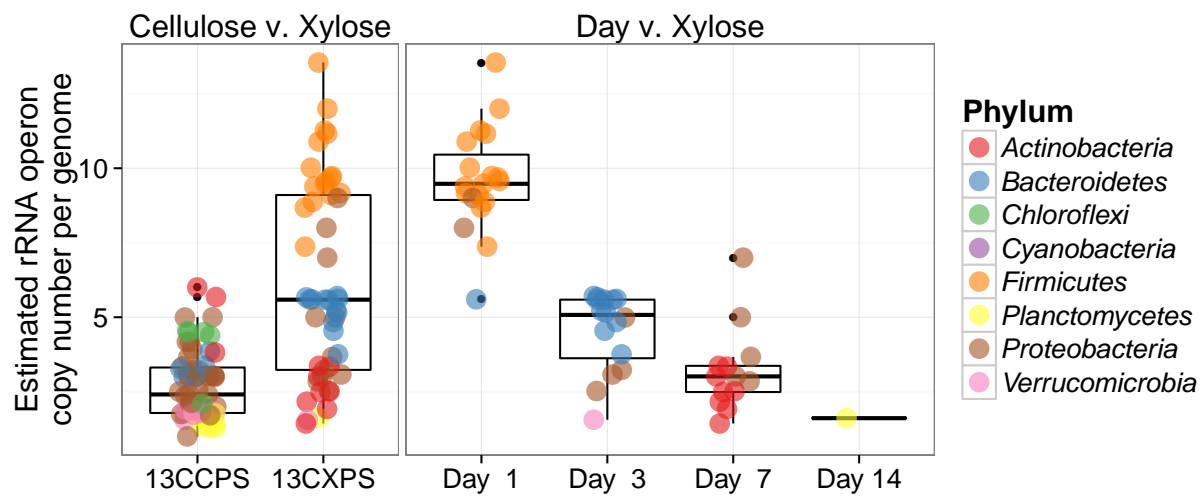


Fig. S1. Estimated rRNA operon copy number per genome for ^{13}C responding OTUs. Panel titles indicate which labeled substrate(s) are depicted.

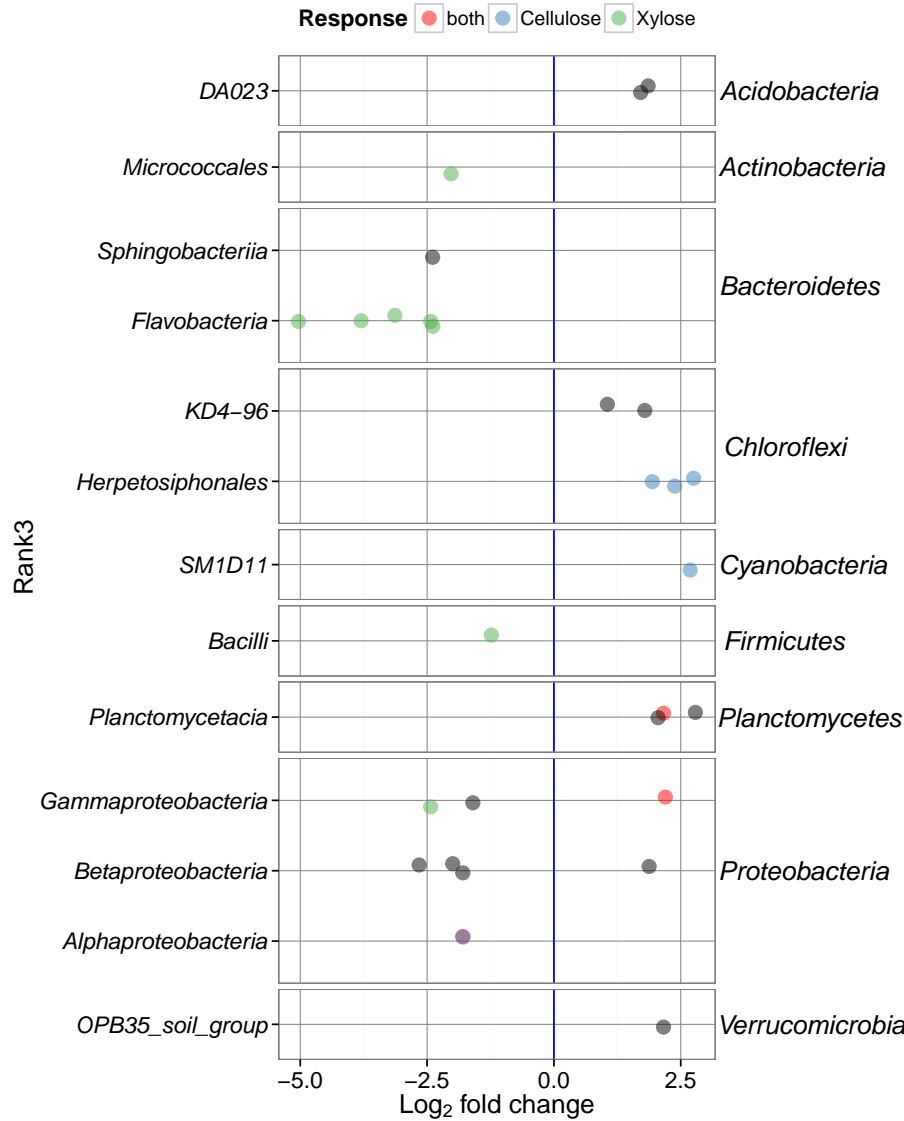


Fig. S2. Fold change time⁻¹ for OTUs that changed significantly in abundance over time. One panel per phylum (phyla indicated on the right). Taxonomic class indicated on the left.

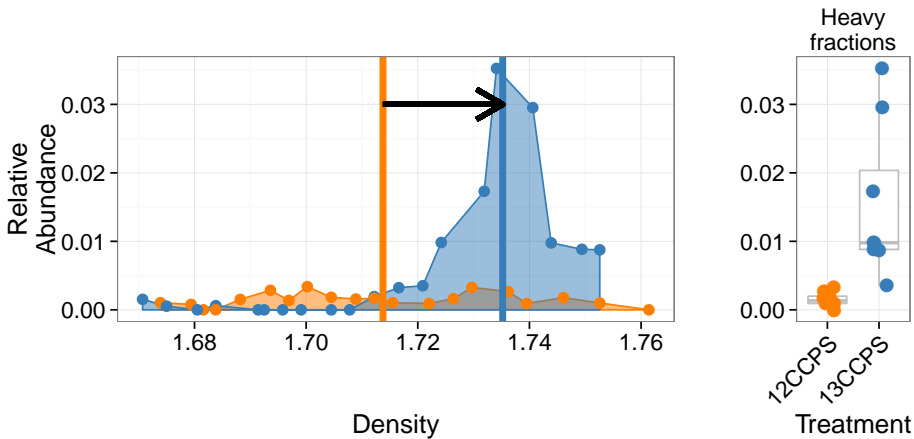


Fig. S3. Density profile for a single ^{13}C -cellulose “responder” OTU in the labeled gradient, blue, and the control gradient, orange. Vertical lines show center of mass for each density profile and arrow denotes the magnitude and direction of the BD shift upon labeling. Panel at right shows relative abundance values in the heavy fractions for each gradient.

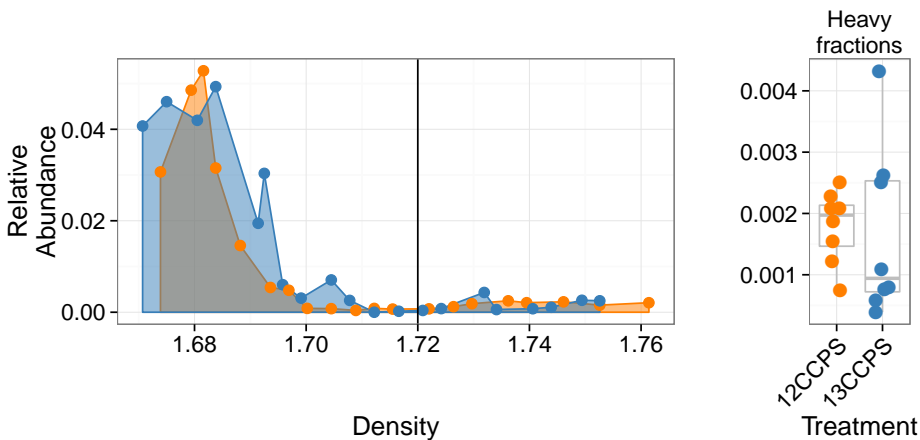


Fig. S4. Density profile for a single ^{13}C -cellulose “non-responder” OTU in the labeled gradient, blue, and the control gradient, orange. Vertical line shows where “heavy” fractions begin as defined in our analysis. Panel at right shows relative abundance values in the heavy fractions for each gradient.

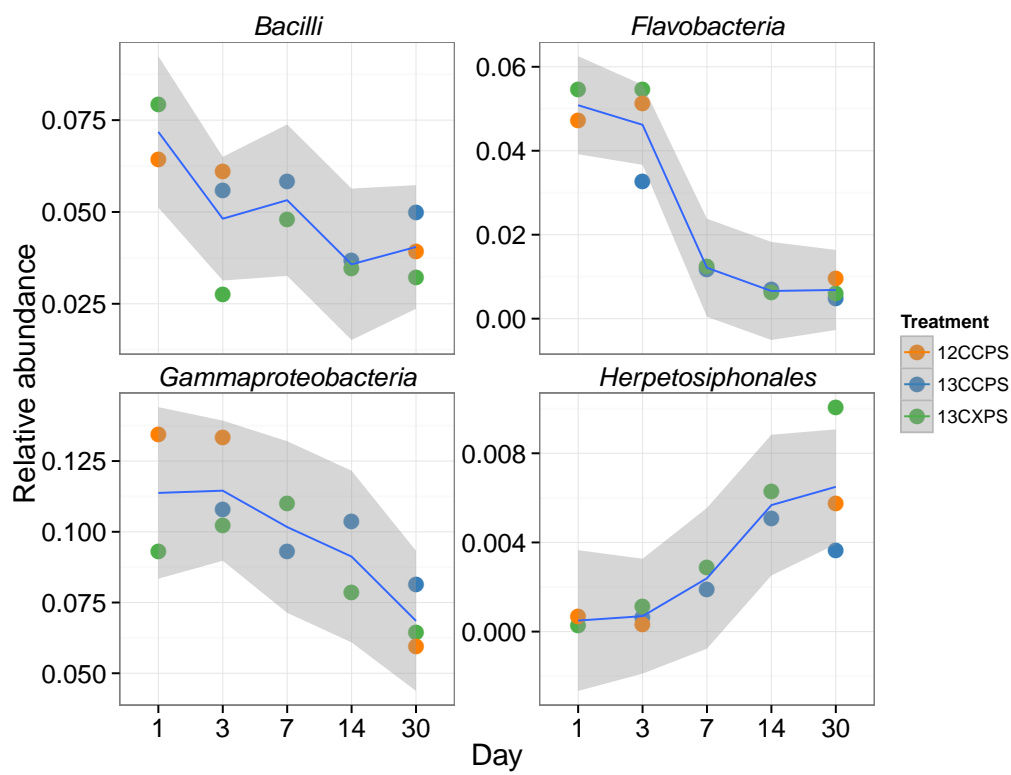


Fig. S5. Relative abundance versus day for classes that changed significantly in relative abundance with time.

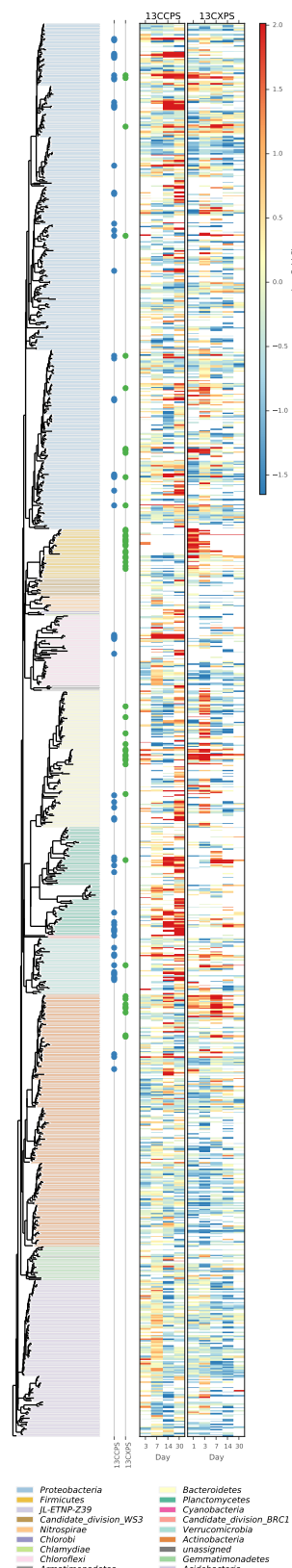


Fig. S6. Phylogenetic tree of sequences passing a user defined sparsity threshold (0.6) for at least one day of the time series. Branches are colored by phylum. ^{13}C -responders for cellulose (blue) and xylose (green) are indicated by a point beside the respective branch. Heatmap demonstrates \log_2 fold change of each taxa through the full time series for both treatments (cellulose, left; xylose, right).

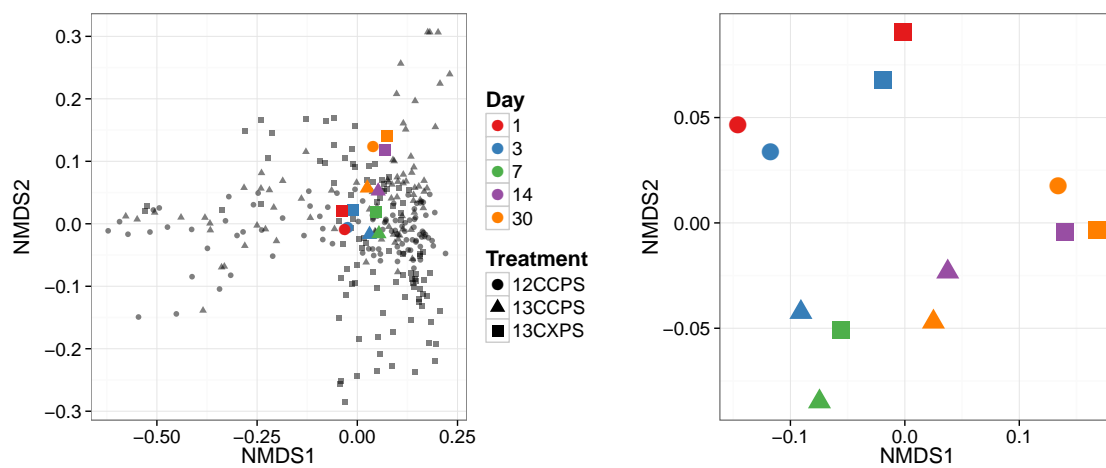
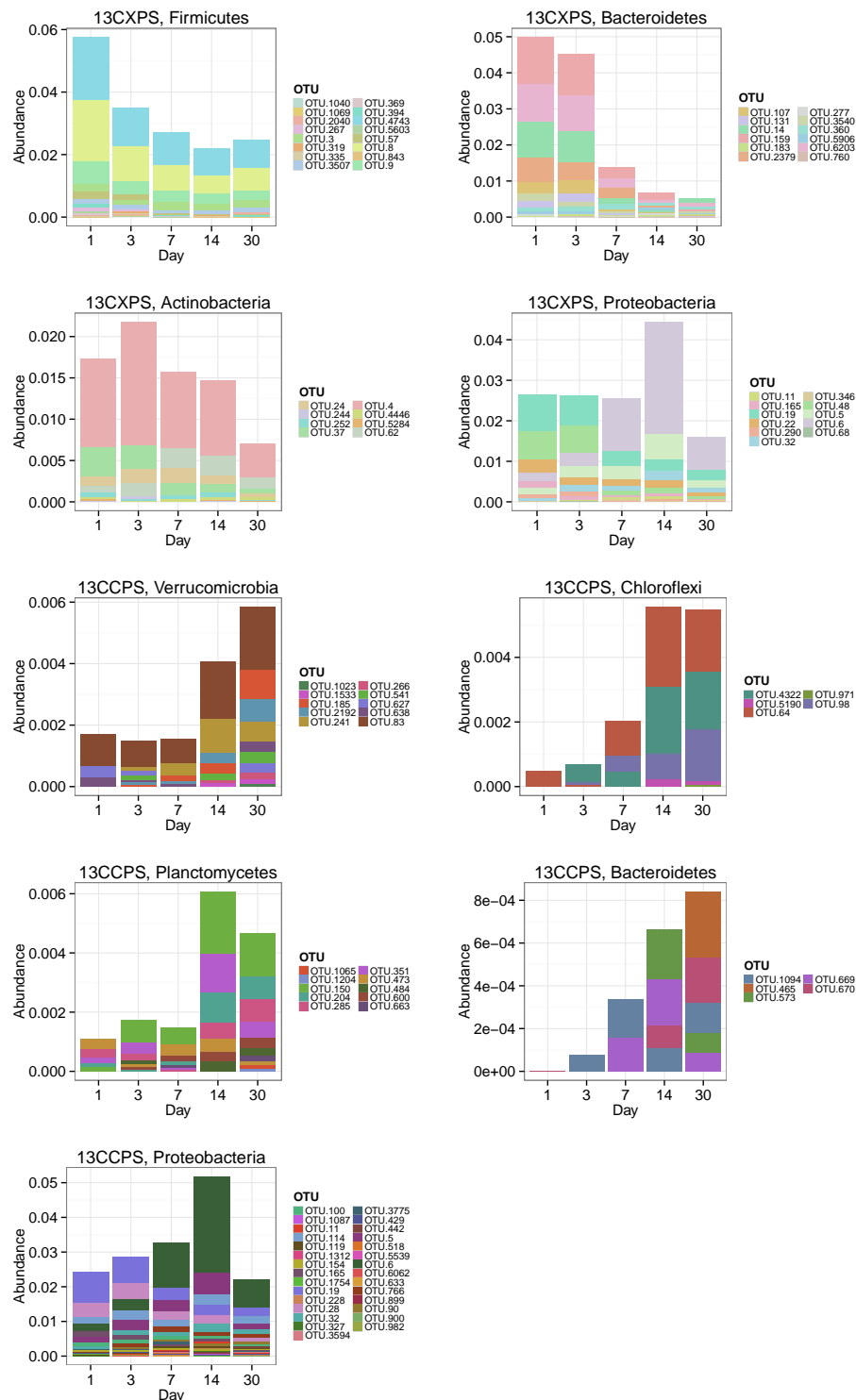


Fig. S7. Ordination of bulk gradient fraction phylogenetic profiles.

**Fig. S8.** Sum of bulk abundances with selected phylum for responder OTUs.

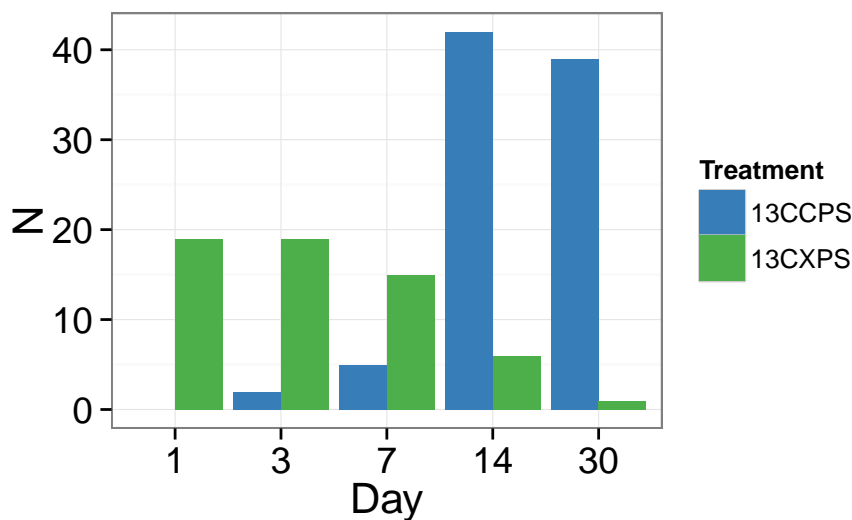


Fig. S9. Counts of responders to each isotopically labeled substrate (cellulose and xylose) over time.

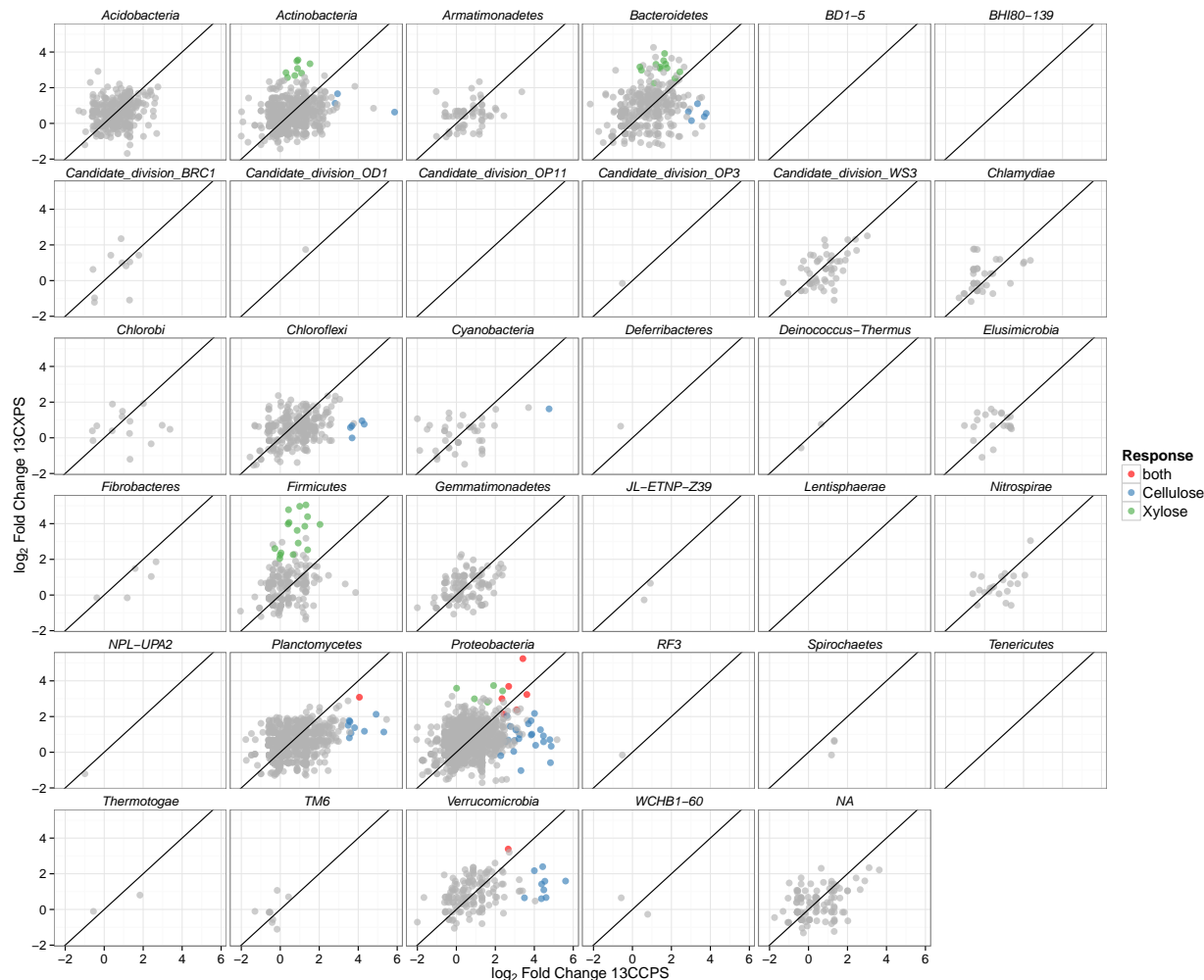


Fig. S10. Maximum \log_2 fold change in response to labeled substrate incorporation for each substrate and all OTUs that pass sparsity filtering in both substrate analyses. Points colored by response. Line has slope of 1 with intercept at the origin. OTUs falling in the top-right quadrant responded to both substrates while those in the top-left and bottom-right responded to ^{13}C -xylose and ^{13}C -cellulose, respectively.

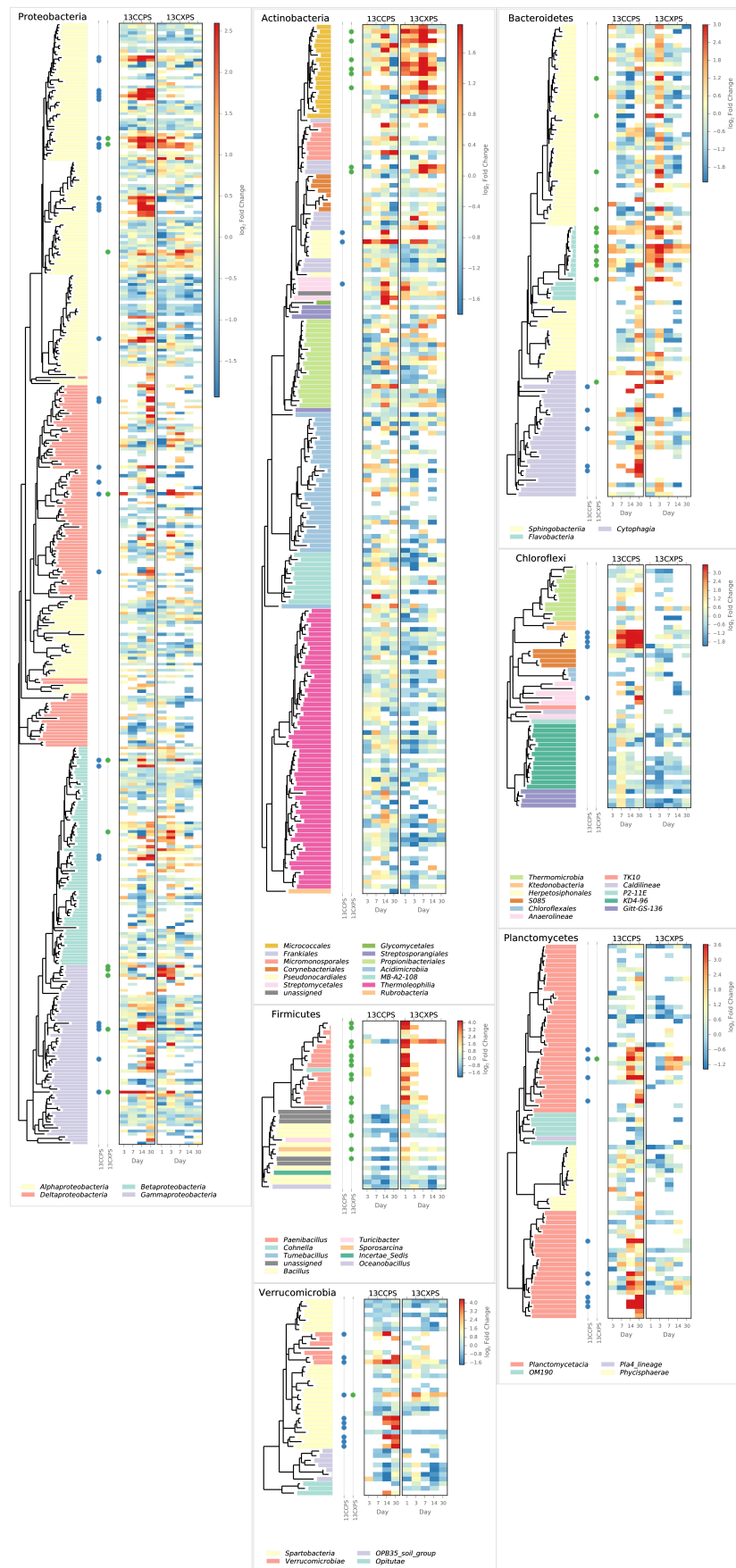


Fig. S11. Phylum specific trees. Heatmap indicates fold change between heavy fractions of control gradients versus labeled gradients. Dots indicate the position of “responders” to ^{13}C -xylose (green) or ^{13}C -cellulose (blue).

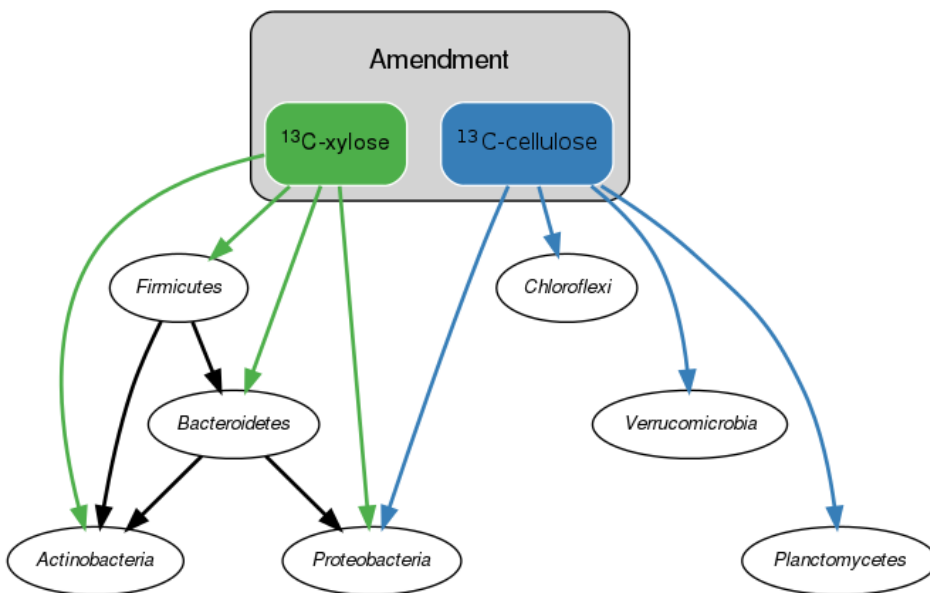


Fig. S12. Conceptual model of soil food web in this experiment.

Table S1: ¹³C-cellulose responders BLAST against Living Tree Project

OTU ID	Fold change ^a	Day ^b	Top BLAST hits	BLAST %ID	Phylum;Class;Order
OTU.862	5.87	14	<i>Allokutzneria albata</i>	100.0	<i>Actinobacteria Pseudonocardiales Pseudonocardiaceae</i>
OTU.257	2.94	14	<i>Lentzea waywayandensis, Lentzea flaviverrucosa</i>	100.0	<i>Actinobacteria Pseudonocardiales Pseudonocardiaceae</i>
OTU.132	2.81	14	<i>Streptomyces spp.</i>	100.0	<i>Actinobacteria Streptomycetales Streptomycetaceae</i>
OTU.465	3.79	30	<i>Ohtaekwangia kribbensis</i>	92.73	<i>Bacteroidetes Cytophagia Cytophagales</i>
OTU.1094	3.69	30	<i>Sporocytophaga myxococcoides</i>	99.55	<i>Bacteroidetes Cytophagia Cytophagales</i>
OTU.669	3.34	30	<i>Ohtaekwangia koreensis</i>	92.69	<i>Bacteroidetes Cytophagia Cytophagales</i>
OTU.573	3.03	30	<i>Adhaeribacter aerophilus</i>	92.76	<i>Bacteroidetes Cytophagia Cytophagales</i>
OTU.670	2.87	30	<i>Adhaeribacter aerophilus</i>	91.78	<i>Bacteroidetes Cytophagia Cytophagales</i>
OTU.971	3.68	30	No hits of at least 90% identity	78.57	<i>Chloroflexi Anaerolineae Anaerolineales</i>
OTU.64	4.31	14	No hits of at least 90% identity	89.5	<i>Chloroflexi Herpetosiphonales Herpetosiphonaceae</i>
OTU.4322	4.19	14	No hits of at least 90% identity	89.14	<i>Chloroflexi Herpetosiphonales Herpetosiphonaceae</i>
OTU.98	3.68	14	No hits of at least 90% identity	88.18	<i>Chloroflexi Herpetosiphonales Herpetosiphonaceae</i>
OTU.5190	3.6	30	No hits of at least 90% identity	88.13	<i>Chloroflexi Herpetosiphonales Herpetosiphonaceae</i>
OTU.120	4.76	14	<i>Vampirovibrio chlorellavorus</i>	94.52	<i>Cyanobacteria SM1D11 uncultured-bacterium</i>
OTU.1065	5.31	14	No hits of at least 90% identity	84.55	<i>Planctomycetes Planctomycetacia Planctomycetales</i>
OTU.484	4.92	14	No hits of at least 90% identity	89.09	<i>Planctomycetes Planctomycetacia Planctomycetales</i>
OTU.1204	4.32	30	<i>Planctomyces limnophilus</i>	91.78	<i>Planctomycetes Planctomycetacia Planctomycetales</i>
OTU.150	4.06	14	No hits of at least 90% identity	86.76	<i>Planctomycetes Planctomycetacia Planctomycetales</i>
OTU.663	3.63	30	<i>Pirellula staleyi DSM 6068</i>	90.87	<i>Planctomycetes Planctomycetacia Planctomycetales</i>
OTU.473	3.58	14	<i>Pirellula staleyi DSM 6068</i>	90.91	<i>Planctomycetes Planctomycetacia Planctomycetales</i>
OTU.285	3.55	30	<i>Blastopirellula marina</i>	90.87	<i>Planctomycetes Planctomycetacia Planctomycetales</i>
OTU.351	3.54	14	<i>Pirellula staleyi DSM 6068</i>	91.86	<i>Planctomycetes Planctomycetacia Planctomycetales</i>
OTU.600	3.48	30	No hits of at least 90% identity	80.37	<i>Planctomycetes Planctomycetacia Planctomycetales</i>
OTU.900	4.87	14	<i>Brevundimonas vesicularis, Brevundimonas nasdae</i>	100.0	<i>Proteobacteria Alphaproteobacteria Caulobacterales</i>
OTU.1754	4.48	14	<i>Asticcacaulis biprosthecum, Asticcacaulis benevestitus</i>	96.8	<i>Proteobacteria Alphaproteobacteria Caulobacterales</i>
OTU.119	3.31	14	<i>Brevundimonas alba</i>	100.0	<i>Proteobacteria Alphaproteobacteria Caulobacterales</i>

Table S1 – continued from previous page

OTU ID	Fold change	Day	Top BLAST hits	BLAST %ID	Phylum;Class;Order
OTU.327	2.99	14	<i>Asticcacaulis biprosthecum,</i> <i>Asticcacaulis benevestitus</i>	98.63	Proteobacteria Alphaproteobacteria Caulobacterales
OTU.982	4.47	14	<i>Devosia neptuniae</i>	100.0	Proteobacteria Alphaproteobacteria Rhizobiales
OTU.1087	4.32	14	<i>Devosia soli</i> , <i>Devosia crocina</i> , <i>Devosia riboflavina</i>	99.09	Proteobacteria Alphaproteobacteria Rhizobiales
OTU.5539	4.01	14	<i>Devosia subaequoris</i>	98.17	Proteobacteria Alphaproteobacteria Rhizobiales
OTU.3775	3.88	14	<i>Devosia glacialis</i> , <i>Devosia chinhatensis</i> , <i>Devosia geojensis</i> , <i>Devosia yakushimensis</i>	98.63	Proteobacteria Alphaproteobacteria Rhizobiales
OTU.429	3.7	30	<i>Devosia limi</i> , <i>Devosia psychrophila</i>	97.72	Proteobacteria Alphaproteobacteria Rhizobiales
OTU.766	3.21	14	<i>Devosia insulae</i>	99.54	Proteobacteria Alphaproteobacteria Rhizobiales
OTU.165	3.1	14	<i>Rhizobium skieniewicense</i> , <i>Rhizobium vignae</i> , <i>Rhizobium larrymoorei</i> , <i>Rhizobium alkalisolii</i> , <i>Rhizobium galegae</i> , <i>Rhizobium huautlense</i>	100.0	Proteobacteria Alphaproteobacteria Rhizobiales
OTU.28	2.59	14	<i>Rhizobium giardinii</i> , <i>Rhizobium tubonense</i> , <i>Rhizobium tibeticum</i> , <i>Rhizobium mesoamericanum CCGE 501</i> , <i>Rhizobium herbae</i> , <i>Rhizobium endophyticum</i>	99.54	Proteobacteria Alphaproteobacteria Rhizobiales
OTU.19	2.44	14	<i>Rhizobium alamii</i> , <i>Rhizobium mesosinicum</i> , <i>Rhizobium mongolense</i> , <i>Arthrobacter viscosus</i> , <i>Rhizobium sullae</i> , <i>Rhizobium yanglingense</i> , <i>Rhizobium loessense</i>	99.54	Proteobacteria Alphaproteobacteria Rhizobiales
OTU.90	2.94	14	<i>Sphingopyxis panaciterrae</i> , <i>Sphingopyxis chilensis</i> , <i>Sphingopyxis sp. BZ30</i> , <i>Sphingomonas sp.</i>	100.0	Proteobacteria Alphaproteobacteria Sphingomonadales
OTU.518	4.8	14	<i>Hydrogenophaga intermedia</i>	100.0	Proteobacteria Betaproteobacteria Burkholderiales
OTU.1312	4.07	30	<i>Paucimonas lemoignei</i>	99.54	Proteobacteria Betaproteobacteria Burkholderiales
OTU.114	2.78	14	<i>Herbaspirillum sp. SUEMI03</i> , <i>Herbaspirillum sp. SUEMI10</i> , <i>Oxalicibacterium solurbis</i> , <i>Herminiumonas fonticola</i> , <i>Oxalicibacterium hortii</i>	100.0	Proteobacteria Betaproteobacteria Burkholderiales
OTU.633	3.84	30	No hits of at least 90% identity	89.5	Proteobacteria Deltaproteobacteria Myxococcales
OTU.3594	3.83	30	<i>Chondromyces robustus</i>	90.41	Proteobacteria Deltaproteobacteria Myxococcales
OTU.442	3.05	30	<i>Chondromyces robustus</i>	92.24	Proteobacteria Deltaproteobacteria Myxococcales
OTU.228	2.54	30	<i>Sorangium cellulosum</i>	98.17	Proteobacteria Deltaproteobacteria Myxococcales

Table S1 – continued from previous page

OTU ID	Fold change	Day	Top BLAST hits	BLAST %ID	Phylum;Class;Order
OTU.899	2.28	30	<i>Enhygromyxa salina</i>	97.72	<i>Proteobacteria Deltaproteobacteria Myxococcales</i>
OTU.6	3.62	7	<i>Cellvibrio fulvus</i>	100.0	<i>Proteobacteria Gammaproteobacteria Pseudomonadales</i>
OTU.6062	4.83	30	<i>Dokdonella sp. DC-3, Luteibacter rhizovicinus</i>	97.26	<i>Proteobacteria Gammaproteobacteria Xanthomonadales</i>
OTU.154	3.24	14	<i>Pseudoxanthomonas mexicana, Pseudoxanthomonas japonensis</i>	100.0	<i>Proteobacteria Gammaproteobacteria Xanthomonadales</i>
OTU.100	2.66	14	<i>Pseudoxanthomonas sacheonensis, Pseudoxanthomonas dokdonensis</i>	100.0	<i>Proteobacteria Gammaproteobacteria Xanthomonadales</i>
OTU.1023	4.61	30	No hits of at least 90% identity	80.54	<i>Verrucomicrobia Spartobacteria Chthoniobacterales</i>
OTU.266	4.54	30	No hits of at least 90% identity	83.64	<i>Verrucomicrobia Spartobacteria Chthoniobacterales</i>
OTU.541	4.49	30	No hits of at least 90% identity	84.23	<i>Verrucomicrobia Spartobacteria Chthoniobacterales</i>
OTU.185	4.37	14	No hits of at least 90% identity	85.14	<i>Verrucomicrobia Spartobacteria Chthoniobacterales</i>
OTU.2192	3.49	30	No hits of at least 90% identity	83.56	<i>Verrucomicrobia Spartobacteria Chthoniobacterales</i>
OTU.1533	3.43	30	No hits of at least 90% identity	82.27	<i>Verrucomicrobia Spartobacteria Chthoniobacterales</i>
OTU.83	5.61	14	<i>Luteolibacter sp. CCTCC AB 2010415</i>	97.72	<i>Verrucomicrobia Verrucomicrobiae Verrucomicrobiales</i>
OTU.627	4.43	14	<i>Verrucomicrobiaceae bacterium DC2a-G7</i>	100.0	<i>Verrucomicrobia Verrucomicrobiae Verrucomicrobiales</i>
OTU.638	4.0	30	<i>Luteolibacter sp. CCTCC AB 2010415, Luteolibacter algae</i>	93.61	<i>Verrucomicrobia Verrucomicrobiae Verrucomicrobiales</i>

^a Maximum observed \log_2 of fold change.^b Day of maximum fold change.

Table S2: ^{13}C -xylose responders BLAST against Living Tree Project

OTU ID	Fold change ^a	Day ^b	Top BLAST hits	BLAST %ID	Phylum;Class;Order
OTU.4446	3.49	7	<i>Catenuloplanes niger</i> , <i>Catenuloplanes castaneus</i> , <i>Catenuloplanes atrovinosus</i> , <i>Catenuloplanes crispus</i> , <i>Catenuloplanes nepalensis</i> , <i>Catenuloplanes japonicus</i>	97.72	Actinobacteria Frankiales Nakamurellaceae
OTU.62	2.57	7	<i>Nakamurella flava</i>	100.0	Actinobacteria Frankiales Nakamurellaceae
OTU.24	2.81	7	<i>Cellulomonas aerilata</i> , <i>Cellulomonas humilata</i> , <i>Cellulomonas terrae</i> , <i>Cellulomonas soli</i> , <i>Cellulomonas xylolytica</i>	100.0	Actinobacteria Micrococcales Cellulomonadaceae
OTU.4	2.84	7	<i>Agromyces ramosus</i>	100.0	Actinobacteria Micrococcales Microbacteriaceae
OTU.37	2.68	7	<i>Phycicola gilvus</i> , <i>Microterricola viridarii</i> , <i>Frigoribacterium faeni</i> , <i>Frondihabitans sp. RS-15</i> , <i>Frondihabitans australicus</i>	100.0	Actinobacteria Micrococcales Microbacteriaceae
OTU.5284	3.56	7	<i>Isoptericola nanjingensis</i> , <i>Isoptericola hypogaeus</i> , <i>Isoptericola variabilis</i>	98.63	Actinobacteria Micrococcales Promicromonosporaceae
OTU.252	3.34	7	<i>Promicromonospora thailandica</i>	100.0	Actinobacteria Micrococcales Promicromonosporaceae
OTU.244	3.08	7	<i>Cellulosimicrobium funkei</i> , <i>Cellulosimicrobium terreum</i>	100.0	Actinobacteria Micrococcales Promicromonosporaceae
OTU.760	2.89	3	<i>Dyadobacter hamtensis</i>	98.63	Bacteroidetes Cytophagia Cytophagales
OTU.14	3.92	3	<i>Flavobacterium oncorhynchi</i> , <i>Flavobacterium glycines</i> , <i>Flavobacterium succinicans</i>	99.09	Bacteroidetes Flavobacteria Flavobacteriales
OTU.6203	3.32	3	<i>Flavobacterium granuli</i> , <i>Flavobacterium glaciei</i>	100.0	Bacteroidetes Flavobacteria Flavobacteriales
OTU.159	3.16	3	<i>Flavobacterium hibernum</i>	98.17	Bacteroidetes Flavobacteria Flavobacteriales
OTU.2379	3.1	3	<i>Flavobacterium pectinovorum</i> , <i>Flavobacterium sp. CS100</i>	97.72	Bacteroidetes Flavobacteria Flavobacteriales
OTU.131	3.07	3	<i>Flavobacterium fluvii</i> , <i>Flavobacterium bacterium HMD1033</i> , <i>Flavobacterium sp. HMD1001</i>	100.0	Bacteroidetes Flavobacteria Flavobacteriales
OTU.3540	2.52	3	<i>Flavobacterium terrigena</i>	99.54	Bacteroidetes Flavobacteria Flavobacteriales
OTU.107	2.25	3	<i>Flavobacterium sp. 15C3</i> , <i>Flavobacterium banpakuense</i>	99.54	Bacteroidetes Flavobacteria Flavobacteriales
OTU.277	3.52	3	<i>Solibius ginsengiterrae</i>	95.43	Bacteroidetes Sphingobacteriia Sphingobacteriales
OTU.183	3.31	3	No hits of at least 90% identity	89.5	Bacteroidetes Sphingobacteriia Sphingobacteriales
OTU.5906	3.16	3	<i>Terrimonas sp. M-8</i>	96.8	Bacteroidetes Sphingobacteriia Sphingobacteriales
OTU.360	2.98	3	<i>Flavisolibacter ginsengisoli</i>	95.0	Bacteroidetes Sphingobacteriia Sphingobacteriales

Table S2 – continued from previous page

OTU ID	Fold change	Day	Top BLAST hits	BLAST %ID	Phylum;Class;Order
OTU.369	5.05	1	<i>Paenibacillus sp. D75,</i> <i>Paenibacillus glycanilyticus</i>	100.0	<i>Firmicutes Bacilli Bacillales</i>
OTU.267	4.97	1	<i>Paenibacillus pabuli,</i> <i>Paenibacillus tundrae,</i> <i>Paenibacillus taichungensis,</i> <i>Paenibacillus xylanexedens,</i> <i>Paenibacillus xylanilyticus</i>	100.0	<i>Firmicutes Bacilli Bacillales</i>
OTU.1040	4.78	1	<i>Paenibacillus daejeonensis</i>	100.0	<i>Firmicutes Bacilli Bacillales</i>
OTU.57	4.39	1	<i>Paenibacillus castaneae</i>	98.62	<i>Firmicutes Bacilli Bacillales</i>
OTU.394	4.06	1	<i>Paenibacillus pocheonensis</i>	100.0	<i>Firmicutes Bacilli Bacillales</i>
OTU.319	3.98	1	<i>Paenibacillus xinjiangensis</i>	97.25	<i>Firmicutes Bacilli Bacillales</i>
OTU.5603	3.96	1	<i>Paenibacillus uliginis</i>	100.0	<i>Firmicutes Bacilli Bacillales</i>
OTU.1069	3.85	1	<i>Paenibacillus terrigena</i>	100.0	<i>Firmicutes Bacilli Bacillales</i>
OTU.843	3.62	1	<i>Paenibacillus agarexedens</i>	100.0	<i>Firmicutes Bacilli Bacillales</i>
OTU.2040	2.91	1	<i>Paenibacillus pectinilyticus</i>	100.0	<i>Firmicutes Bacilli Bacillales</i>
OTU.3	2.61	1	[<i>Brevibacterium</i>] <i>frigoritolerans</i> , <i>Bacillus sp. LMG 20238</i> , <i>Bacillus coahuilensis m4-4</i> , <i>Bacillus simplex</i>	100.0	<i>Firmicutes Bacilli Bacillales</i>
OTU.335	2.53	1	<i>Paenibacillus thailandensis</i>	98.17	<i>Firmicutes Bacilli Bacillales</i>
OTU.3507	2.36	1	<i>Bacillus spp.</i>	98.63	<i>Firmicutes Bacilli Bacillales</i>
OTU.8	2.26	1	<i>Bacillus niaci</i>	100.0	<i>Firmicutes Bacilli Bacillales</i>
OTU.4743	2.24	1	<i>Lysinibacillus fusiformis</i> , <i>Lysinibacillus sphaericus</i>	99.09	<i>Firmicutes Bacilli Bacillales</i>
OTU.9	2.04	1	<i>Bacillus megaterium</i> , <i>Bacillus flexus</i>	100.0	<i>Firmicutes Bacilli Bacillales</i>
OTU.22	2.8	7	<i>Paracoccus sp. NB88</i>	99.09	<i>Proteobacteria Alphaproteobacteria Rhodobacterales</i>
OTU.5	3.69	7	<i>Delftia tsuruhatensis</i> , <i>Delftia lacustris</i>	100.0	<i>Proteobacteria Betaproteobacteria Burkholderiales</i>
OTU.346	3.44	3	<i>Pseudoduganella violaceinigra</i>	99.54	<i>Proteobacteria Betaproteobacteria Burkholderiales</i>
OTU.32	3.0	3	<i>Sandaracinus amyloyticus</i>	94.98	<i>Proteobacteria Deltaproteobacteria Myxococcales</i>
OTU.68	3.74	7	<i>Shigella flexneri</i> , <i>Escherichia fergusonii</i> , <i>Escherichia coli</i> , <i>Shigella sonnei</i>	100.0	<i>Proteobacteria Gammaproteobacteria Enterobacteriales</i>
OTU.290	3.59	1	<i>Pantoea spp.</i> , <i>Kluyvera spp.</i> , <i>Klebsiella spp.</i> , <i>Erwinia spp.</i> , <i>Enterobacter spp.</i> , <i>Buttiauxella spp.</i>	100.0	<i>Proteobacteria Gammaproteobacteria Enterobacteriales</i>
OTU.11	5.25	7	<i>Stenotrophomonas pavani</i> , <i>Stenotrophomonas maltophilia</i> , <i>Pseudomonas geniculata</i>	99.54	<i>Proteobacteria Gammaproteobacteria Xanthomonadales</i>
OTU.48	2.99	1	<i>Aeromonas spp.</i>	100.0	<i>Proteobacteria Gammaproteobacteria aaa34a10</i>
OTU.241	3.38	3	No hits of at least 90% identity	87.73	<i>Verrucomicrobia Spartobacteria Chthoniobacteriales</i>

^a Maximum observed \log_2 of fold change.^b Day of maximum fold change.